NACA RM L55L30

C2

NACA

RESEARCH MEMORANDUM

FOR REFERENCE

NOT TO BE TAKEN FROM THIS ROOM

EFFECTS OF LEADING-EDGE RADIUS ON THE LONGITUDINAL STABILITY CHARACTERISTICS OF TWO 60° SWEPTBACK WINGS AT HIGH REYNOLDS NUMBERS

By William C. Schneider

Langley Aeronautical Laboratory
Langley Field, Va.

CLASSIFICATION CHANGED

To UNCLASSIFIED

NACA Res Ltr

By authority of NRN-123 Date effective Dec 13, 1957

AMT 1-21-58

CLASSIFIED DOCUMENT

This material contains information affecting the National Defense of the United States within the meaning of the espionage laws, Title 18, U.S.C., Secs. 793 and 794, the transmission or revelation of which in any manner to an unauthorized person is prohibited by law.

NATIONAL ADVISORY COMMITTEE FOR AERONAUTICS

WASHINGTON

March 19, 1956

NACA RM L55L30

NATIONAL ADVISORY COMMITTEE FOR AERONAUTICS

RESEARCH MEMORANDUM

EFFECTS OF LEADING-EDGE RADIUS ON THE LONGITUDINAL STABILITY CHARACTERISTICS OF TWO 60° SWEPTBACK WINGS AT HIGH REYNOLDS NUMBERS

By William C. Schneider

SUMMARY

Tests have been completed on two 60° sweptback wings of aspect ratios 2 and 3 to provide further information on the influence of leading-edge radius on the static longitudinal stability characteristics of swept wings. These tests are a continuation of those reported in NACA RM L55F06 and RM L55H04. The wings had symmetrical 9-percent-thick airfoil sections parallel to the root chord with leading-edge radii of 0.89 percent of the chord or 1.30 percent of the chord. The wings were tested at Reynolds numbers from 1.4×10^6 to 10.4×10^6 and at Mach numbers from 0.05 to 0.30.

Little effect on the inflection lift coefficient was noted when the leading-edge radius was increased, for wings of both aspect ratios. Small Reynolds number effects were found for the wings of aspect ratio 3, and only slightly larger effects were noted for the wings of aspect ratio 2. No appreciable Mach number effect was found in the range of these tests.

INTRODUCTION

As part of an investigation of the effects of changes in leading-edge radius, aspect ratio, sweepback, and Reynolds numbers on the static longitudinal stability characteristics of swept wings (refs. 1 and 2), tests have been made on two 60° sweptback wings of aspect ratios of 2 and 3 with varying leading-edge radii. The airfoil sections parallel to the airstream were NACA 0009-63 and NACA 0009-(7.25)3 which have leading-edge radii of 0.0089c and 0.0130c, respectively, in planes parallel to the airstream.

Tests were conducted at tunnel pressures of 14.7 and 33 pounds per square inch absolute, which permitted ranges of Reynolds number from

1.4×10^6 to 6.44×10^6 ($M = 0.063$ to $M = 0.302$) and 2.27×10^6 to 10.40×10^6 ($M = 0.046$ to $M = 0.202$), respectively.

SYMBOLS

$C_{L_{inf_s}}$	inflection lift coefficient, stable change in pitching moment $\left(-\frac{dC_m}{dC_L}\right)$ increasing
$C_{L_{inf_u}}$	inflection lift coefficient, unstable change in pitching moment $\left(-\frac{dC_m}{dC_L}\right)$ decreasing
C_L	lift coefficient, $\frac{\text{Lift}}{qS}$
C_m	pitching-moment coefficient about 0.25c, $\frac{\text{Pitching moment}}{qS\bar{c}}$
$C_{L_{max}}$	maximum lift coefficient
A	aspect ratio, b^2/S
b	wing span, ft
c	local wing chord parallel to plane of symmetry, ft
$\bar{c}$	mean aerodynamic chord, $\frac{1}{S}\int_{-b/2}^{b/2} c^2 dy$, ft
M	Mach number
q	free-stream dynamic pressure, $\frac{1}{2}\rho V^2$, lb/sq ft
R	Reynolds number
S	wing area, sq ft
V	free-stream velocity, ft/sec
x	chordwise ordinate of airfoil section, ft

y	spanwise coordinate normal to plane of symmetry, ft
z	vertical ordinate of airfoil section, ft
α	wing angle of attack, deg
$\Lambda_{c/4}$	sweepback of the quarter-chord line
ρ	density of air, slugs/cu ft

MODEL

The wings tested (fig. 1) during this investigation had the following geometric characteristics:

Wing	$\Lambda_{c/4}$	A	Taper ratio	Leading-edge radius	Airfoil section
1	60°	3	0.500	0.0089c	NACA 0009-63
2	60°	2	.636	.0089c	NACA 0009-63
3	60°	3	.500	.0130c	NACA 0009-(7.25)3
4	60°	2	.636	.0130c	NACA 0009-(7.25)3

It should be pointed out that wings 2 and 4 were made from wings 1 and 3, respectively, by removing the wing tips. Thus, the taper ratio for the wings of aspect ratio 2 differed from that of the wings of aspect ratio 3.

The NACA four-digit series airfoil section (parallel to the air stream) was chosen since there was a systematic procedure for varying the leading-edge radius, keeping the location and magnitude of the maximum thickness constant (ref. 3). The airfoil contours were carefully constructed so that the airfoil sections are believed to be quite accurate. Particular emphasis was placed on the leading edge where the contour is believed to have been within 0.005 inch (about 0.02 percent chord).

It can be seen from the airfoil ordinates listed on figure 1, that the entire nose shape is altered when the leading-edge radius is changed. However, the leading-edge radius is a convenient means of identifying the airfoil section and is used as such throughout this paper.

TESTS AND CORRECTIONS

Tests

Tests were conducted at tunnel pressures of 14.7 and 33 pounds per square inch absolute through a large part of the tunnel speed range. This permitted Reynolds number and Mach number variations as follows:

Tunnel pressure, lb/sq in. abs	R		M	
	A = 3	A = 2	A = 3	A = 2
14.7	1.41×10^6 to 6.32×10^6	1.50×10^6 to 6.44×10^6	0.063 to 0.302	0.067 to 0.284
33	2.27×10^6 to 9.75×10^6	2.52×10^6 to 10.40×10^6	0.046 to 0.202	0.049 to 0.202

The model was supported on the normal two-support system of the 19-foot pressure tunnel.

Corrections

The pitching-moment data and values of angle of attack have been corrected for tunnel-wall effects by the method of reference 4. These corrections are as follows:

for the wings of aspect ratio 3

$$\Delta\alpha = 0.967C_L$$

$$\Delta C_m = 0.00392C_L$$

for the wings of aspect ratio 2

$$\Delta\alpha = 0.755C_L$$

$$\Delta C_m = 0.00158C_L$$

Since the primary interest in these data was centered on the variation of the lift and pitching moment rather than on the absolute values, tests

to determine the model support tare and interference effects were not made. However, the zero-lift pitching-moment coefficient and the angle of attack at zero lift are an indication of the combined effects of model support tare and interference, airstream misalinement, and model asymmetry. Assuming these corrections to be independent of lift coefficient, the lift and pitching-moment curves were shifted by the values of the zero-lift pitching moment and angle of attack as a first-order approximation.

[redacted]

The variations of lift and pitching-moment coefficients with angle of attack are presented on figures 2 and 3 for the wings of aspect ratio 3 and on figures 4 and 5 for the wings of aspect ratio 2. The variation of pitching moment with lift coefficient is presented on figures 6 and 7 and figures 8 and 9 for the wings of aspect ratio 3 and 2, respectively.

The effects of leading-edge radius on the pitching-moment characteristics of the wings of aspect ratios 3 and 2 are illustrated on figures 10 and 11, while the effects of Reynolds number on the two wings are shown on figures 12 and 13. Mach number effects are shown on figures 14 and 15 for the wings under examination.

The variations of $C_{L_{inf_u}}$ and $C_{L_{inf_s}}$ with Reynolds number are shown on figure 16 for the wings of aspect ratio 3 and on figure 17 for the wings of aspect ratio 2. The quantities $C_{L_{inf_u}}$ and $C_{L_{inf_s}}$ are used to designate the lift coefficient beyond which there is a marked change in the pitching-moment characteristics, $C_{L_{inf_u}}$ designating an unstable change, and $C_{L_{inf_s}}$ designating a stable change. For the wing of aspect ratio 3, two curves of $C_{L_{inf_u}}$ are shown since two unstable breaks occur. The pitching-moment curves, of course, show two stable breaks as well. Only the first and strongest break has been plotted on the figure.

Increasing the leading-edge radius had little effect on $C_{L_{inf_s}}$ or $C_{L_{inf_u}}$ for either the wings of aspect ratio 3 or 2 (see figs. 16 and 17) although the trend for the wings of aspect ratio 2 was towards an increase in $C_{L_{inf}}$ with an increase in radius (see ref. 1).

[redacted]

An examination of the pitching-moment variations for the two wings (compare figs. 6 and 8 and figs. 7 and 9) indicates that the changes in loading (as lift coefficient is changed) are more abrupt for the wing of aspect ratio 3 than for the wing of aspect ratio 2.

The value of $C_{L_{inf_s}}$ showed little change as Reynolds number was varied (figs. 16 and 17) for either wing. However, for the wings of aspect ratio 3 (of both radii), some significant slope changes occurred at higher angles of attack as the Reynolds number was increased (fig. 12), a fact which indicated that while the initial point of increase in lift was not affected by changes in Reynolds number, the rate of growth (with lift) of the increase was affected. The pitching-moment curves for the wings of aspect ratio 2 (fig. 13) do not show this dependence upon Reynolds number.

No significant Mach number effect was found for either wing (figs. 14 and 15) through the range of Mach numbers tested (up to $M = 0.30$).

Langley Aeronautical Laboratory,
National Advisory Committee for Aeronautics,
Langley Field, Va., December 7, 1955.

[redacted]

REFERENCES

1. Foster, Gerald V., and Schneider, William C.: Effects of Leading-Edge Radius on the Longitudinal Stability of Two 45° Sweptback Wings As Influenced by Reynolds Numbers up to 8.20×10^6 and Mach Numbers up to 0.303. NACA RM L55F06, 1955.

2. Foster, Gerald V.: Effects of Leading-Edge Radius on the Longitudinal Stability of Two 45° Sweptback Wings Incorporating Leading-Edge Camber as Influenced by Reynolds Numbers up to 8.00×10^6 and Mach Numbers up to 0.290. NACA RM L55H04, 1955.

3. Abbott, Ira H., and von Doenhoff, Albert E.: Theory of Wing Sections. McGraw-Hill Book Company, Inc., 1949.

4. Sivells, James C., and Salmi, Rachel M.: Jet-Boundary Corrections for Complete and Semispan Swept Wings in Closed Circular Wind Tunnels. NACA TN 2454, 1951.

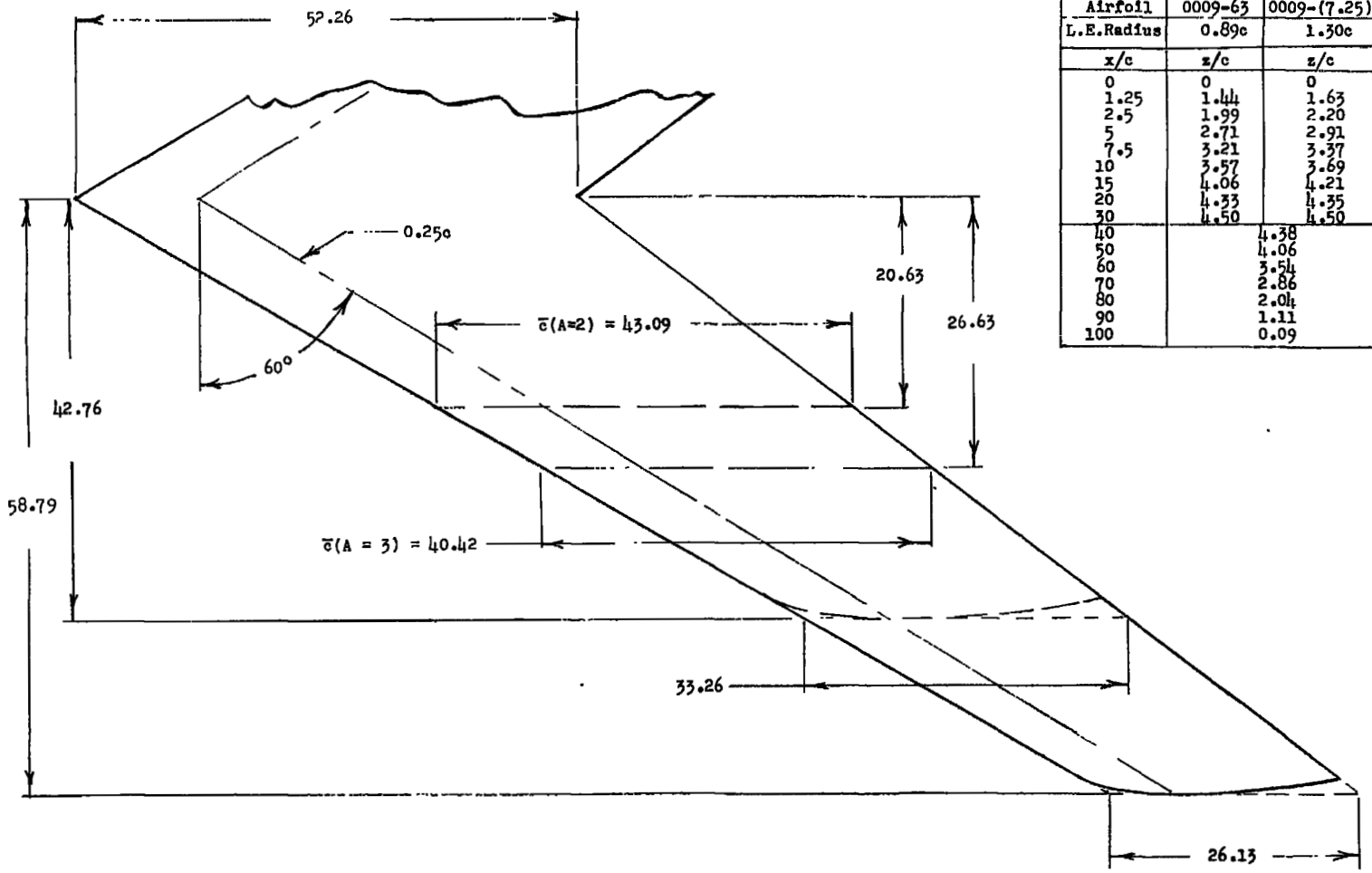

Section Coordinates in Percent		
Airfoil	0009-63	0009-(7.25)-3
L.E.Radius	0.89c	1.30c
x/c	z/c	z/c
0	0	0
1.25	1.44	1.63
2.5	1.99	2.20
5	2.71	2.91
7.5	3.21	3.37
10	3.57	3.69
15	4.06	4.21
20	4.33	4.35
30	4.50	4.50
40	4.38	
50	4.06	
60	3.54	
70	2.86	
80	2.04	
90	1.11	
100	0.09	

Figure 1.- Details of the wings. All dimensions given in inches unless otherwise noted.

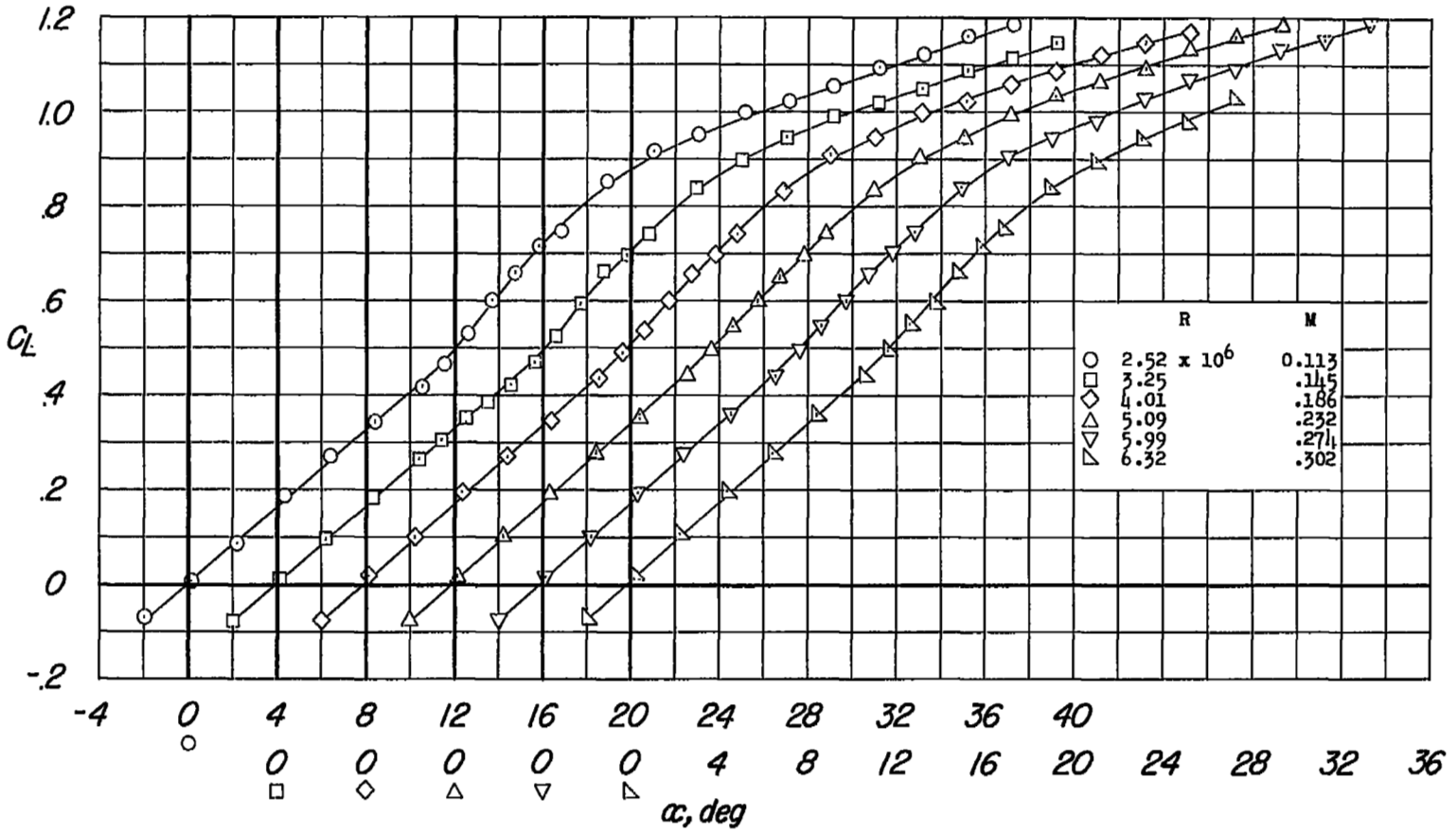

(a) C_L against α; atmospheric pressure.

Figure 2.- Variation of lift and pitching-moment coefficients of a 60° swept-back wing with angle of attack. Aspect ratio 3; leading-edge radius 0.0130c.

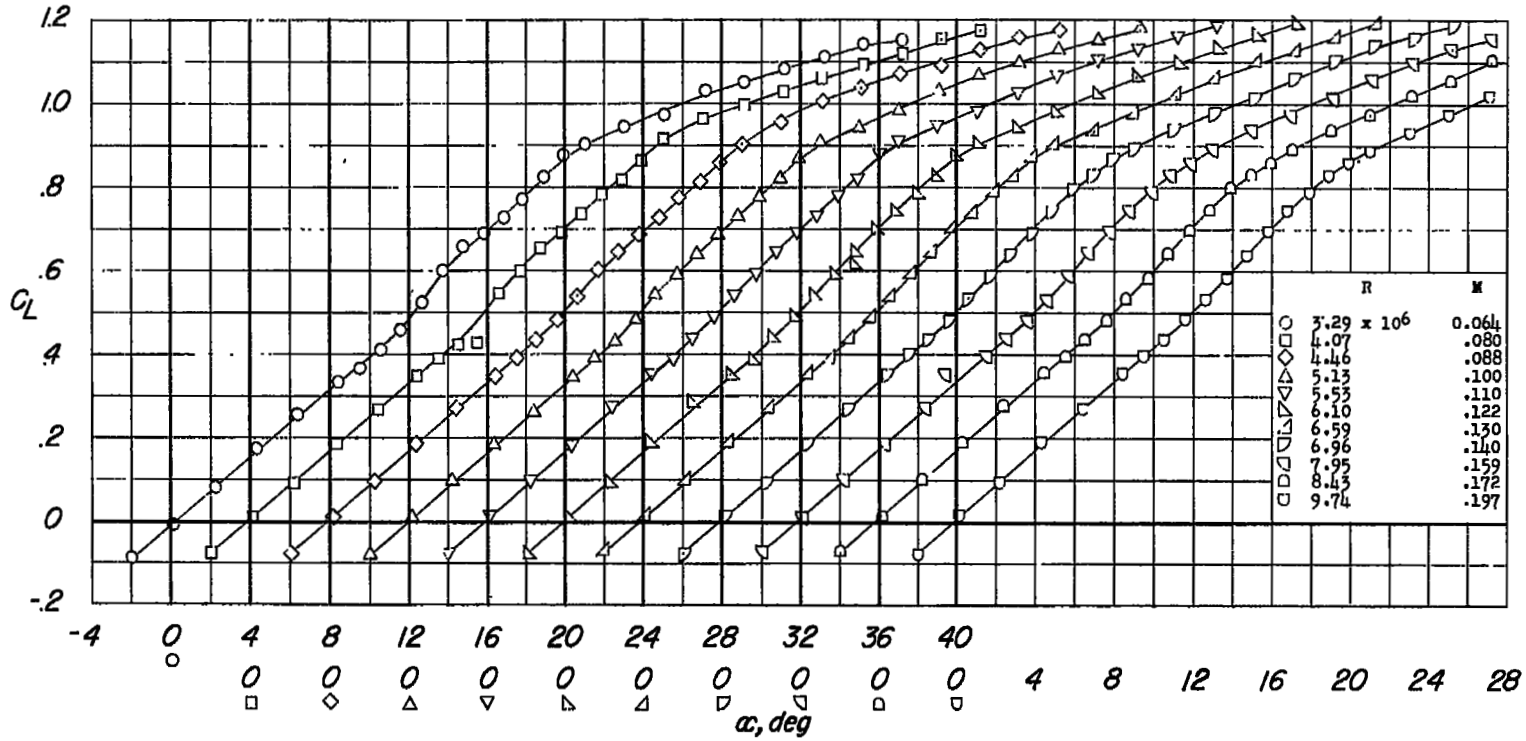

(b) C_L against α; pressure, 33 pounds per square inch.

Figure 2.- Continued.

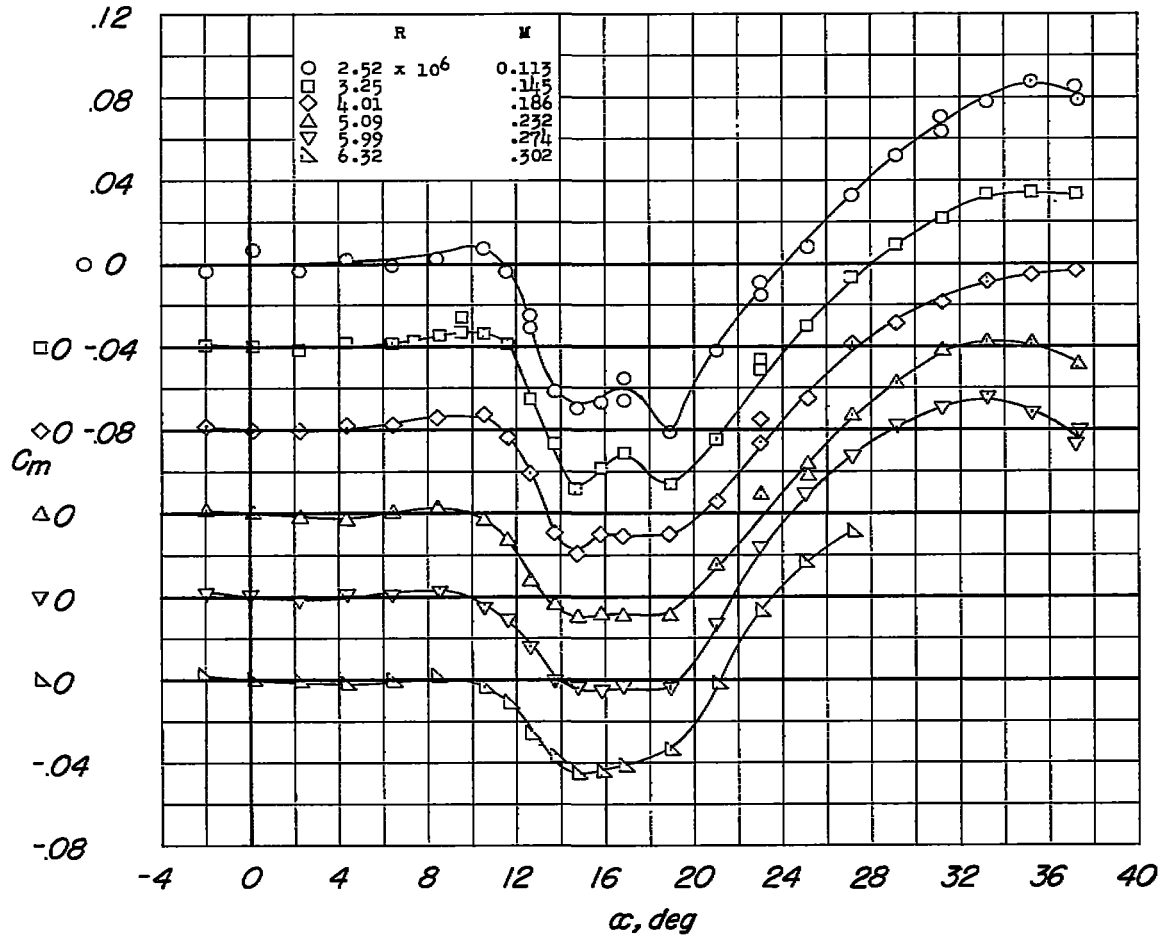

(c) C_m against α; atmospheric pressure.

Figure 2.- Continued.

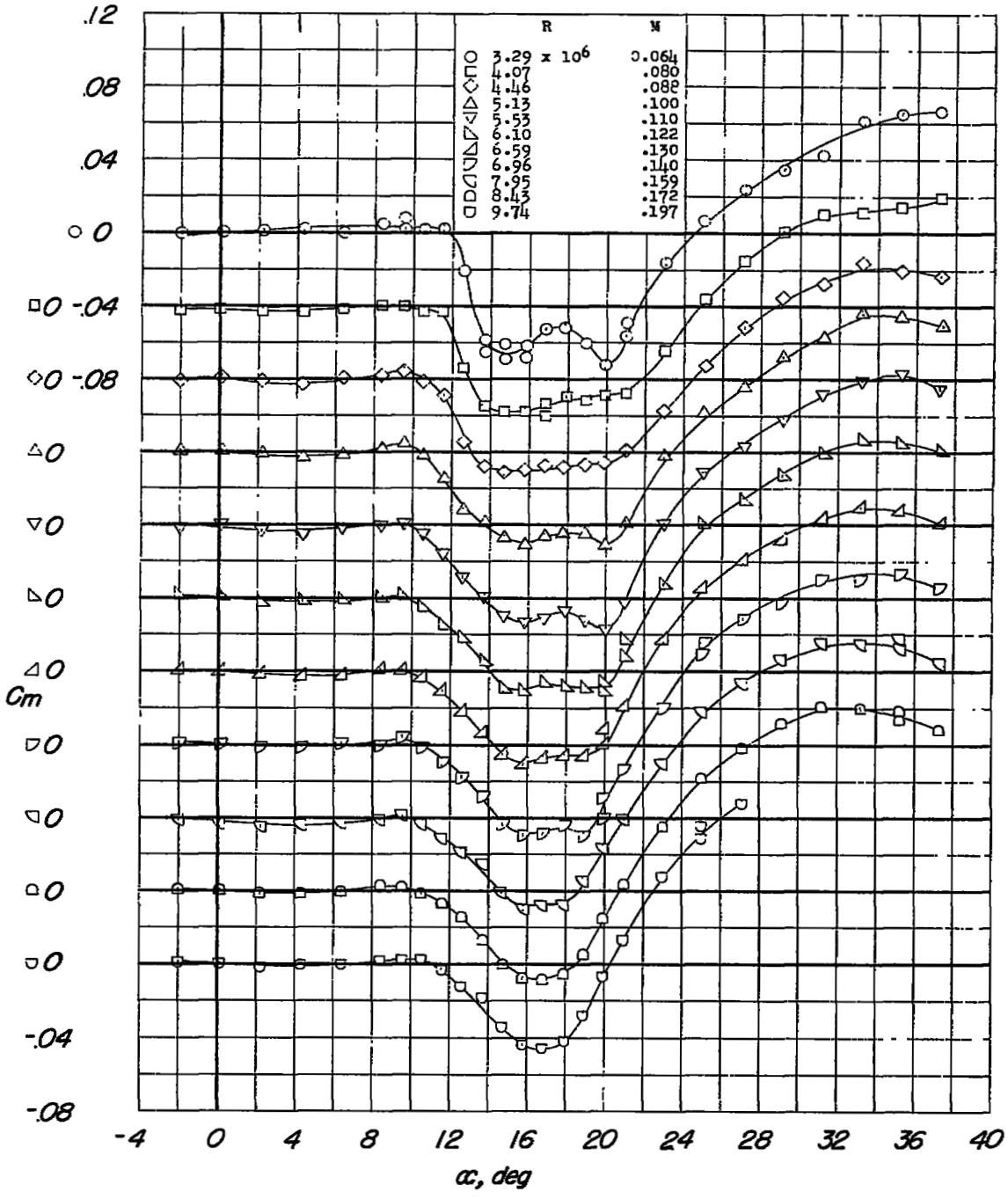

(d) C_m against α; pressure, 33 pounds per square inch.

Figure 2.- Concluded.

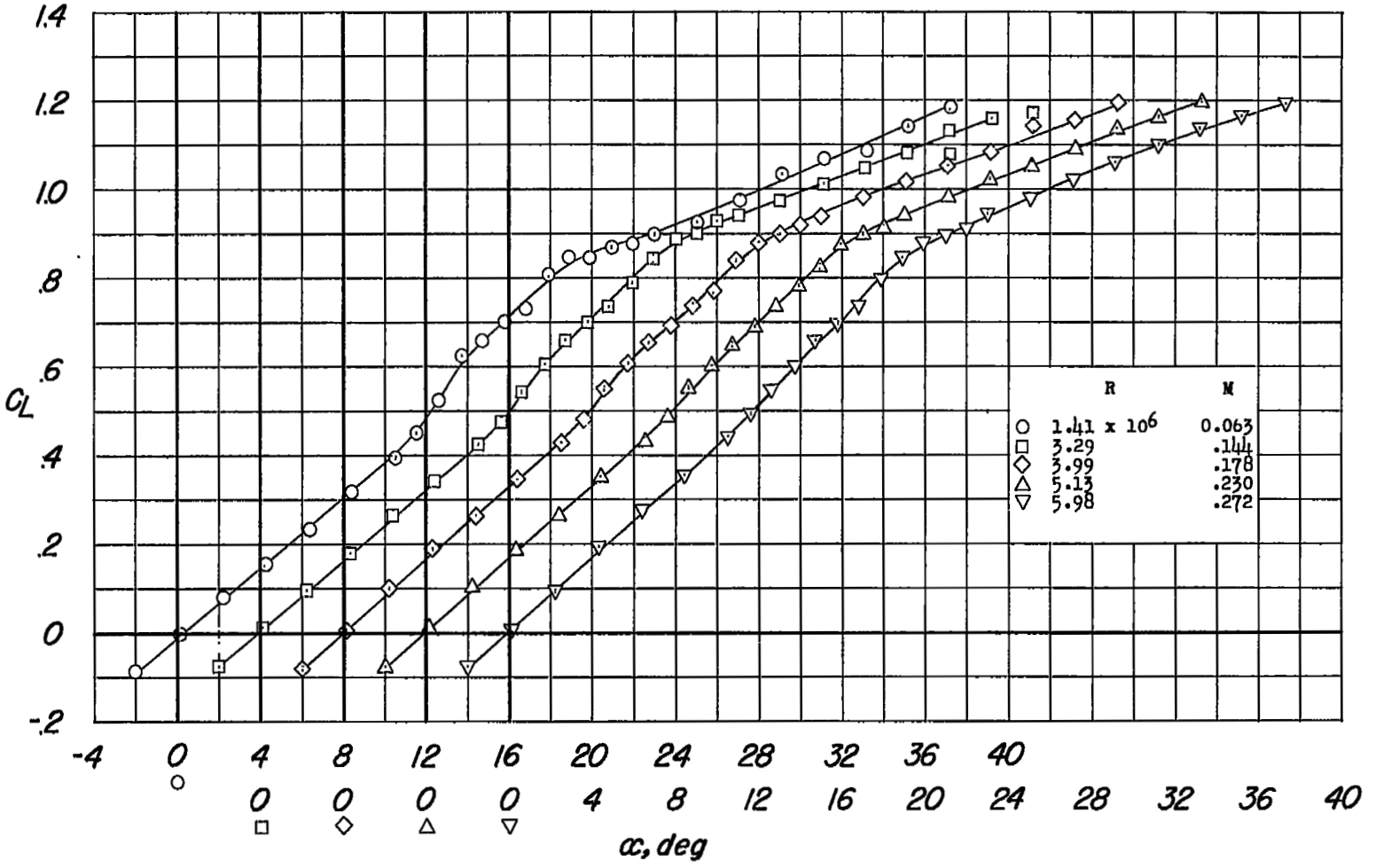

(a) C_L against α; atmospheric pressure.

Figure 3.- Variation of lift and pitching-moment coefficients of a 60° swept-back wing with angle of attack. Aspect ratio 3; leading-edge radius 0.0089c.

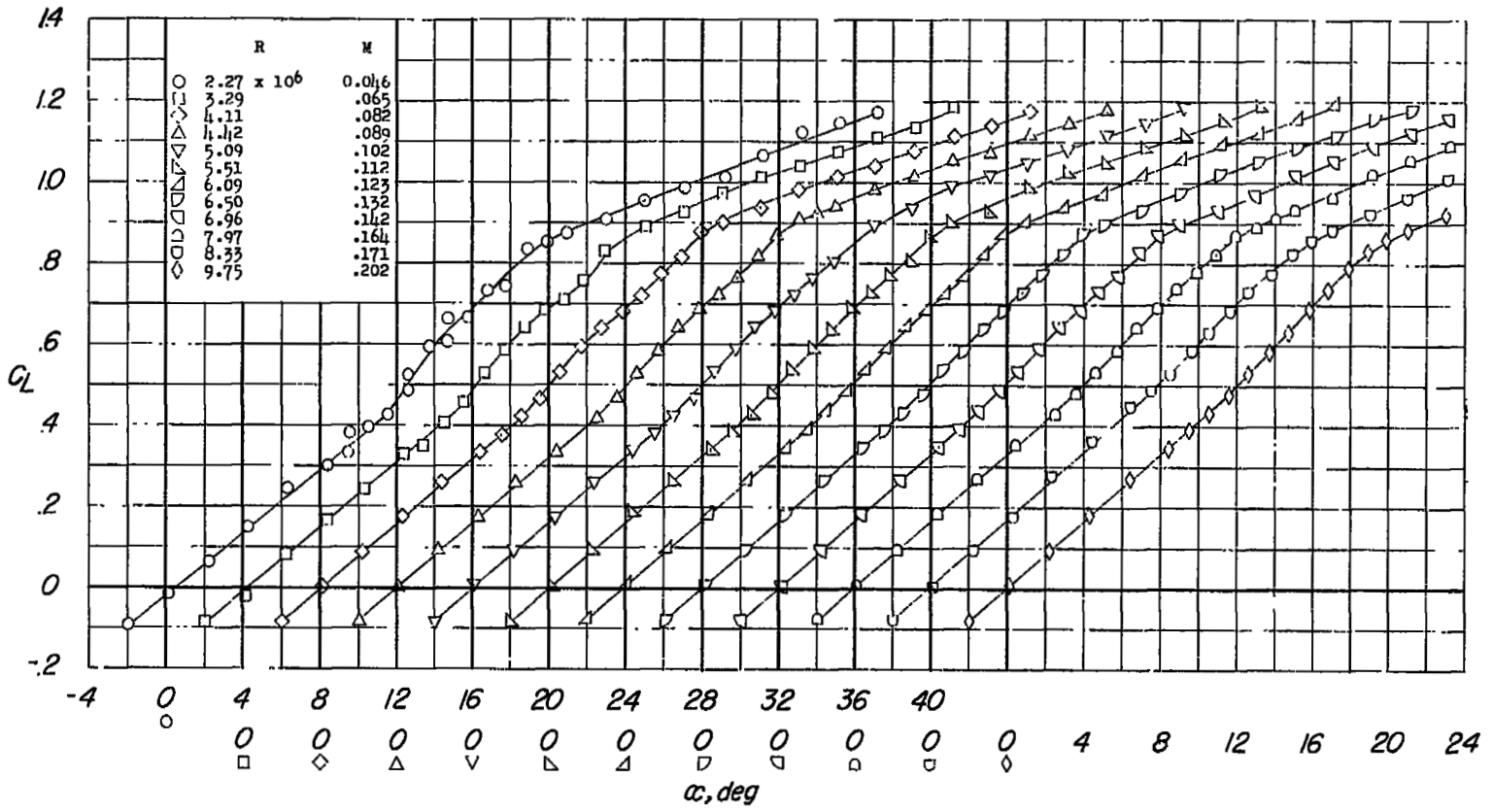

(b) C_L against α; pressure, 33 pounds per square inch.

Figure 3.- Continued.

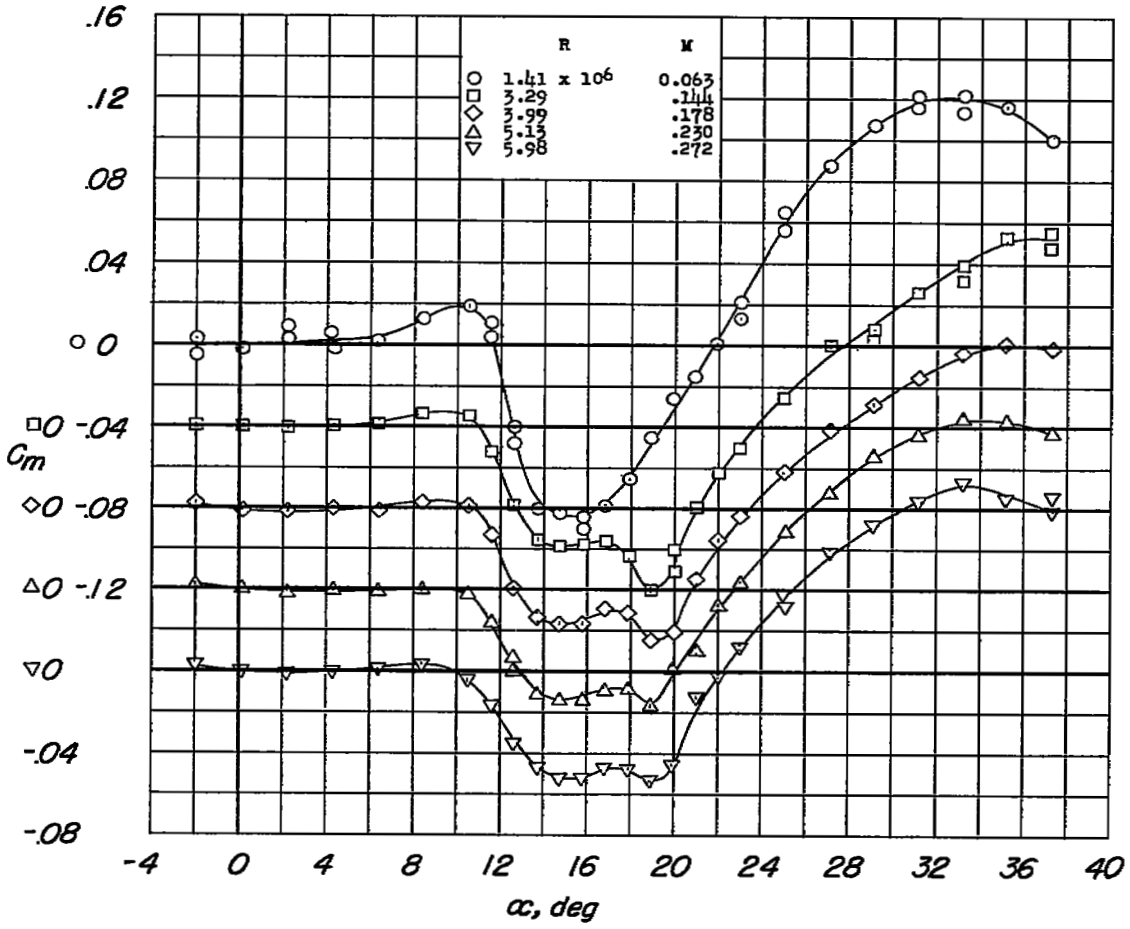

(c) C_m against α; atmospheric pressure.

Figure 3.- Continued.

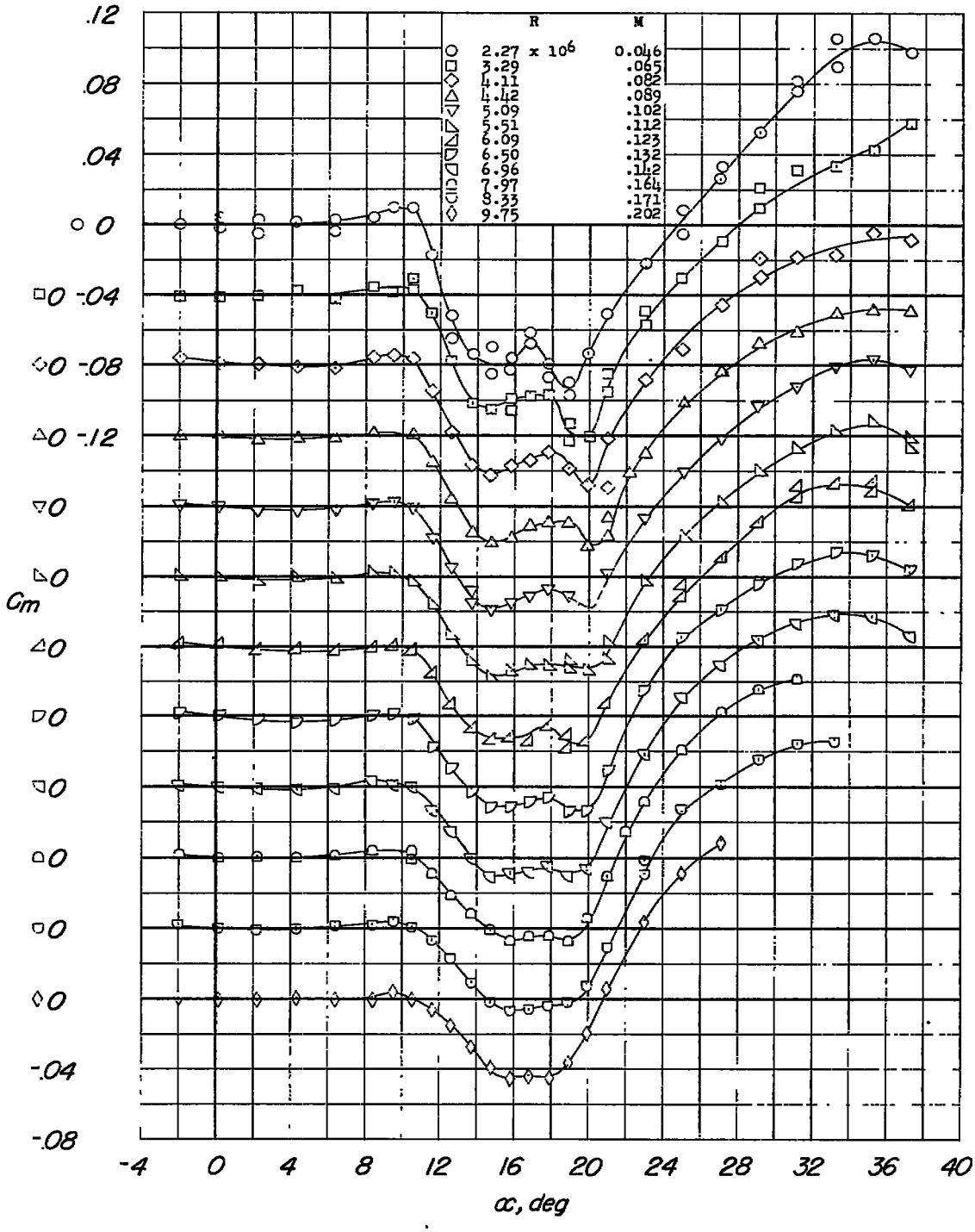

(d) C_m against α; pressure, 33 pounds per square inch.

Figure 3.- Concluded.

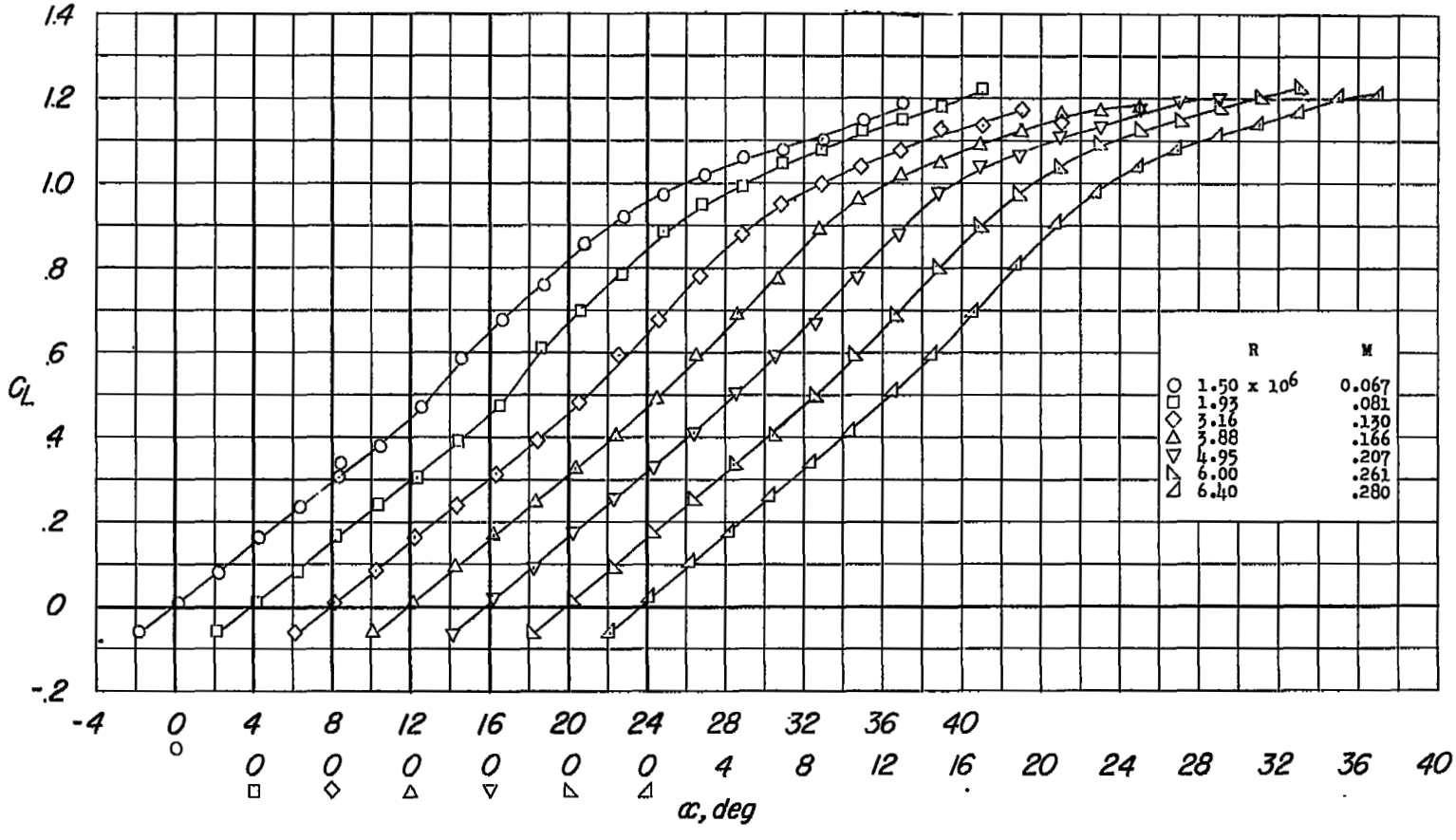

(a) C_L against α; atmospheric pressure.

Figure 4.- Variation of lift and pitching-moment coefficients of a 60° swept-back wing with angle of attack. Aspect ratio 2; leading-edge radius 0.0130c.

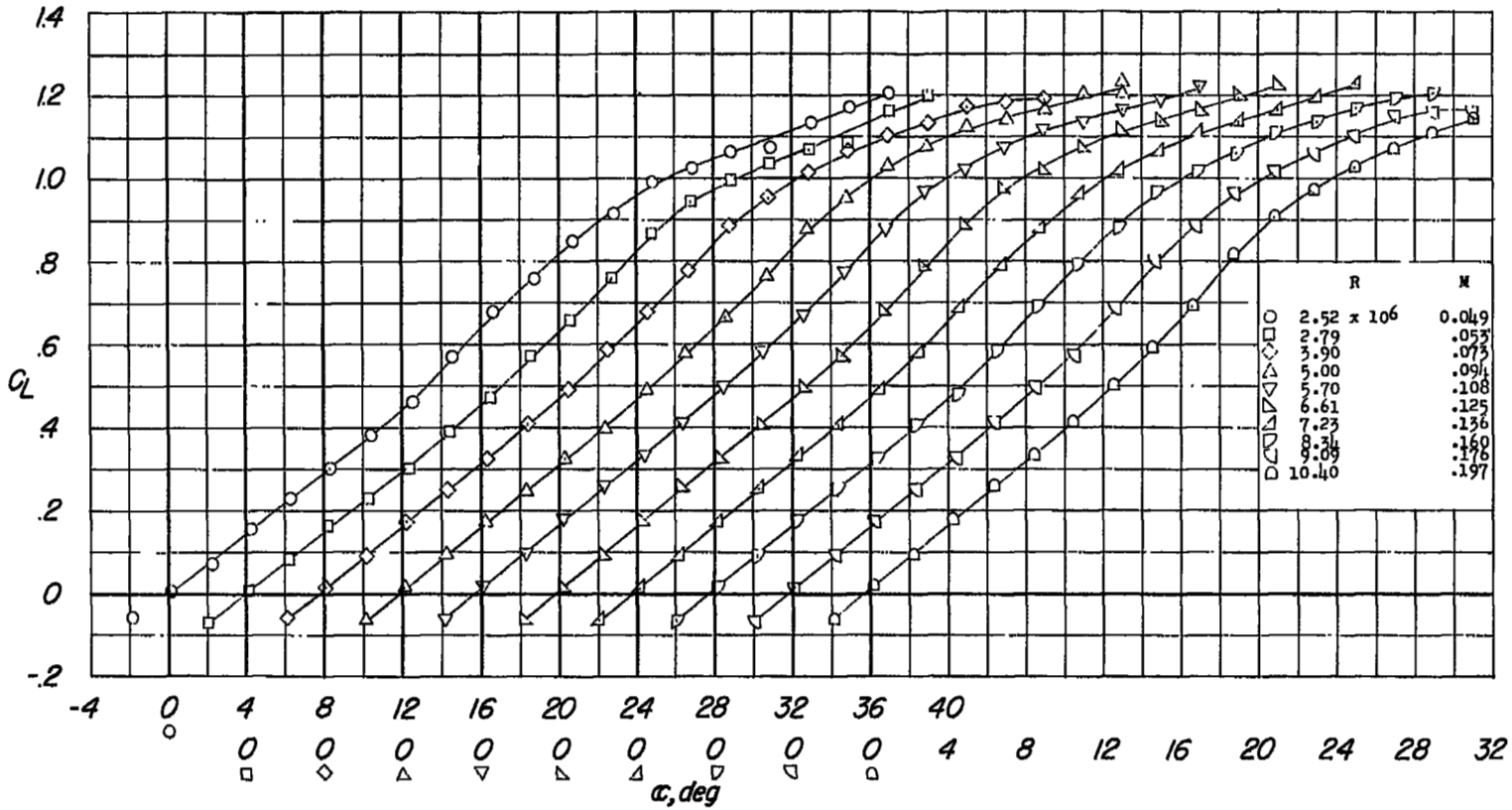

(b) C_L against α; pressure, 33 pounds per square inch.

Figure 4.- Continued.

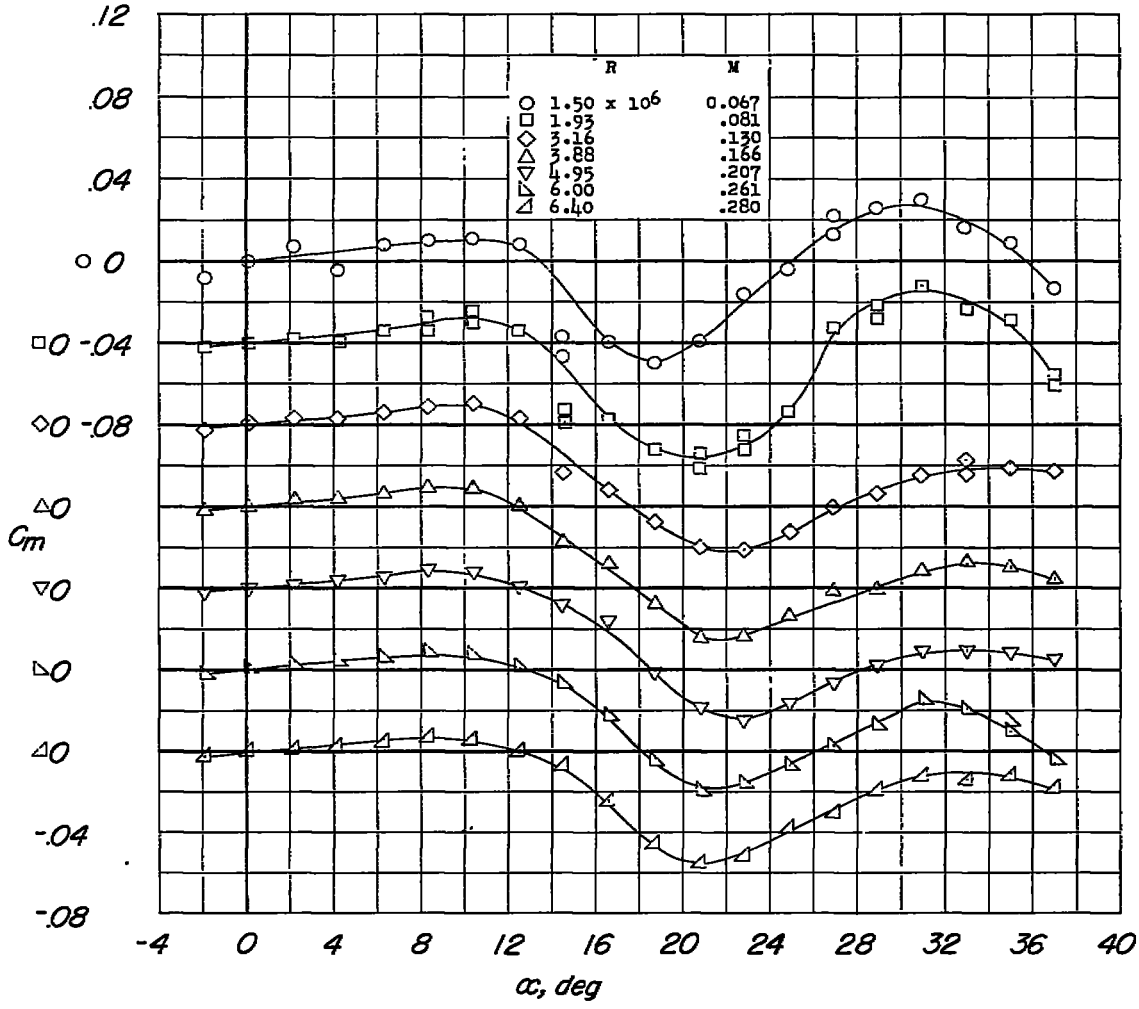

(c) C_m against α; atmospheric pressure.

Figure 4.- Continued.

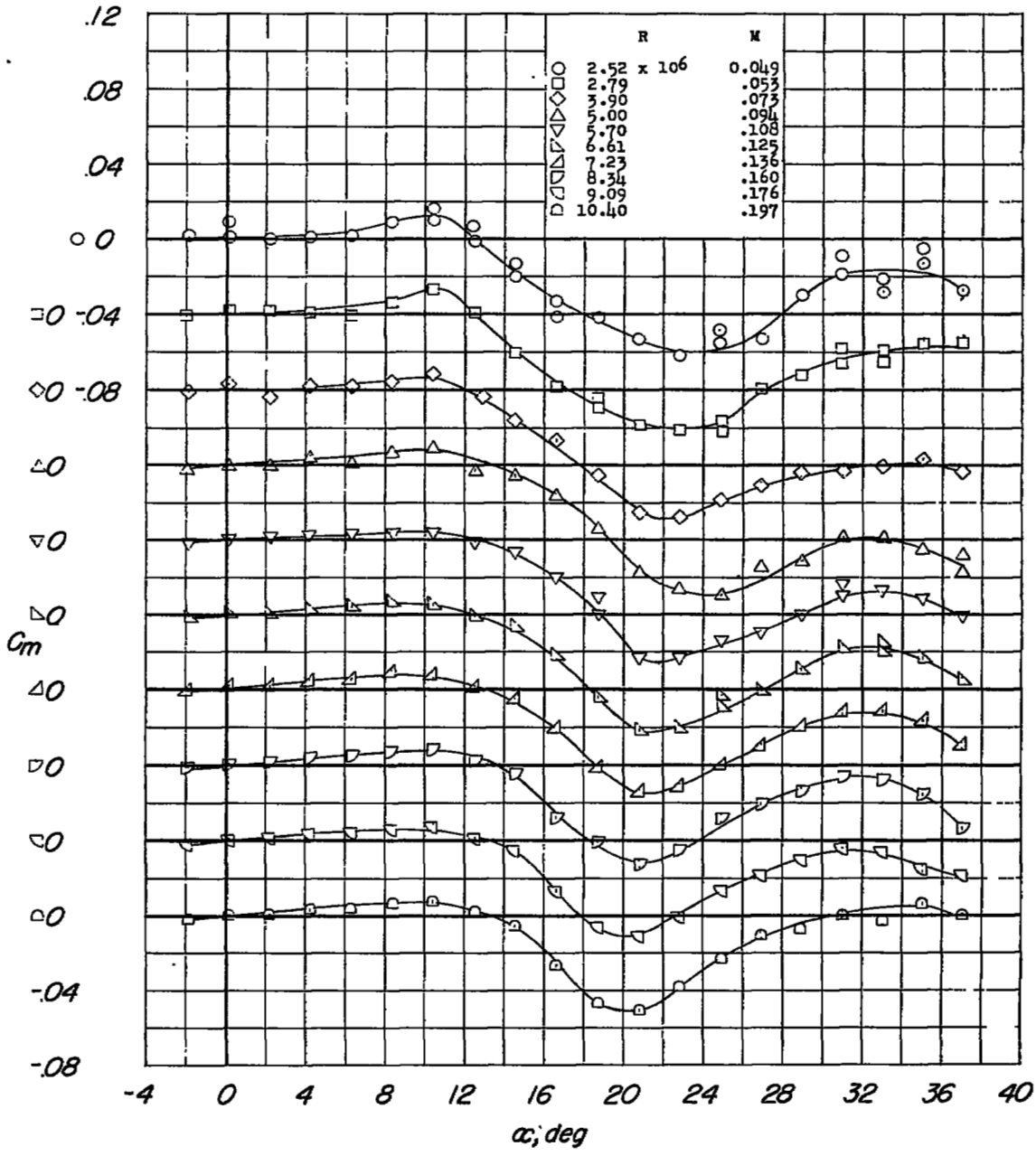

(d) C_m against α; pressure, 33 pounds per square inch.

Figure 4.- Concluded.

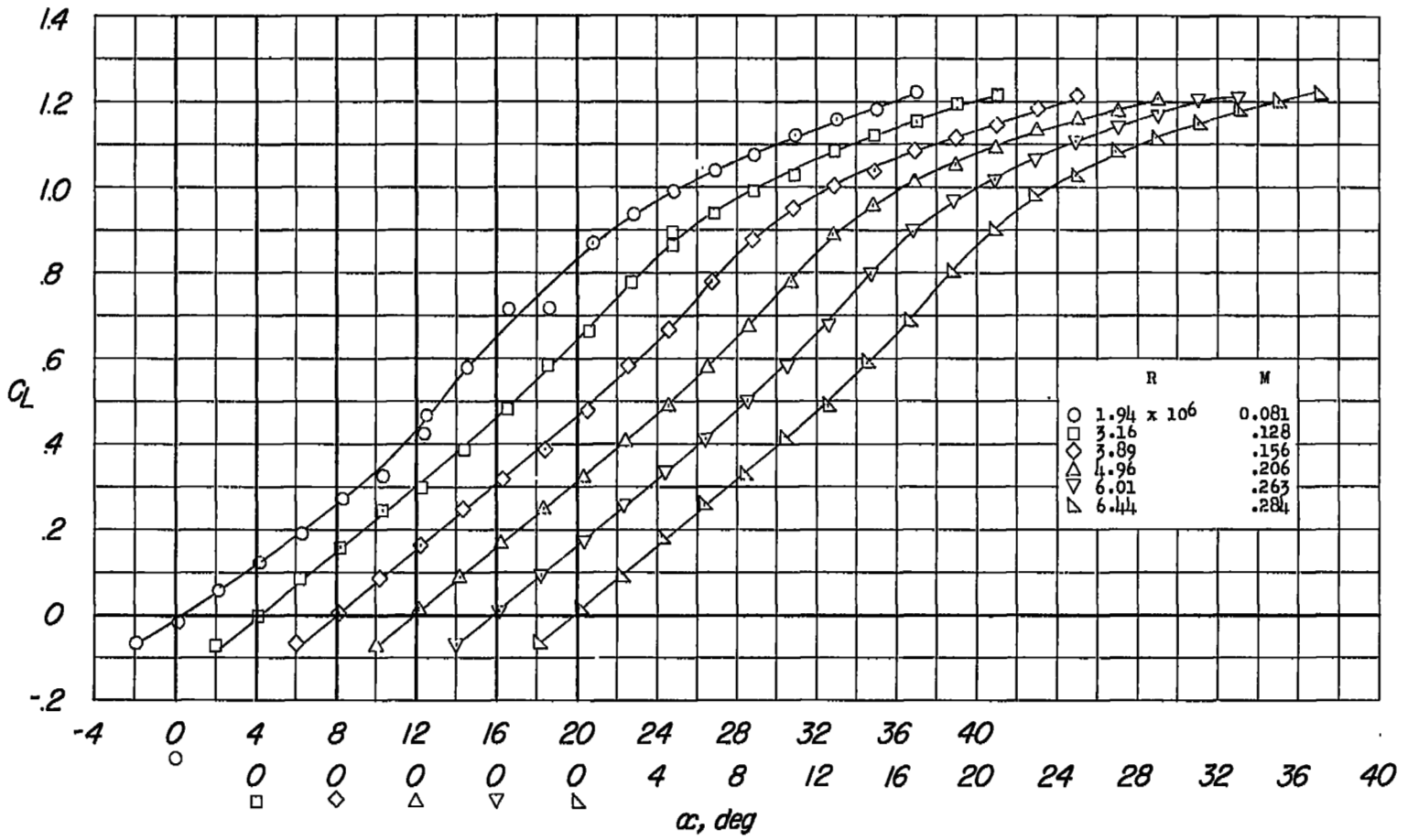

(a) C_L against α; atmospheric pressure.

Figure 5.- Variation of lift and pitching-moment coefficients of a 60° swept-back wing with angle of attack. Aspect ratio 2; leading-edge radius 0.0089c.

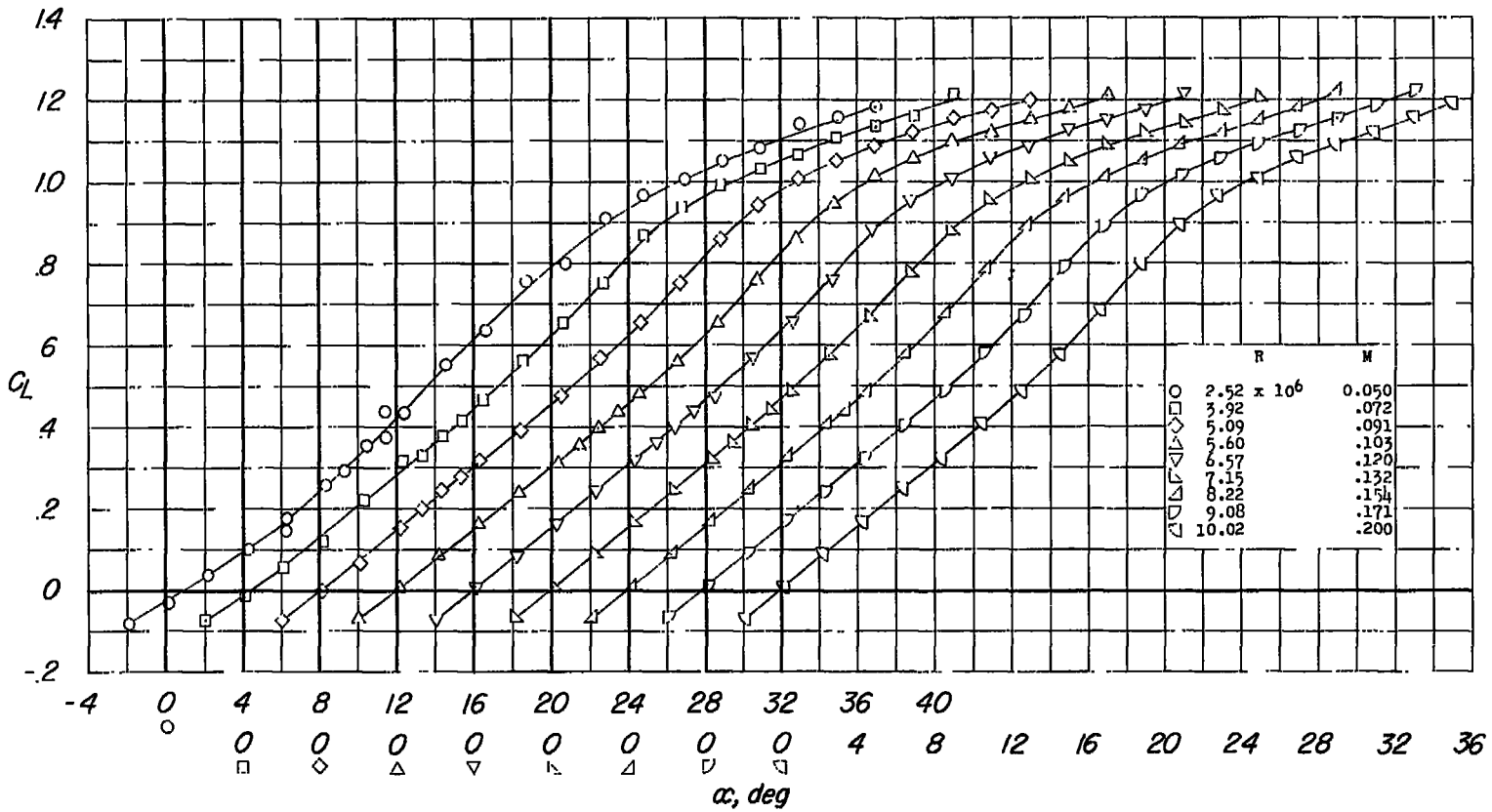

(b) C_L against α; pressure, 33 pounds per square inch.

Figure 5.- Continued.

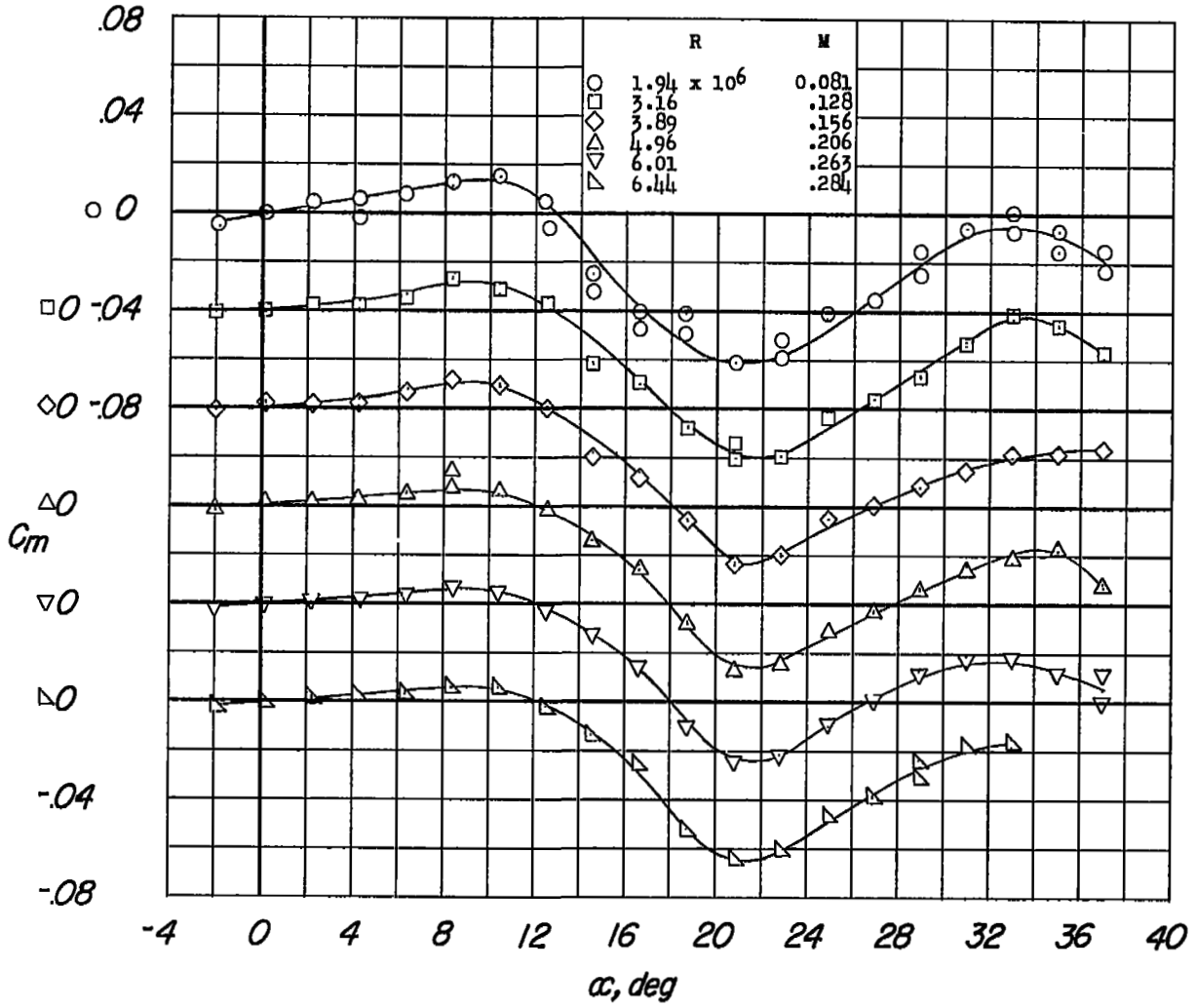

(c) C_m against α; atmospheric pressure.

Figure 5.- Continued.

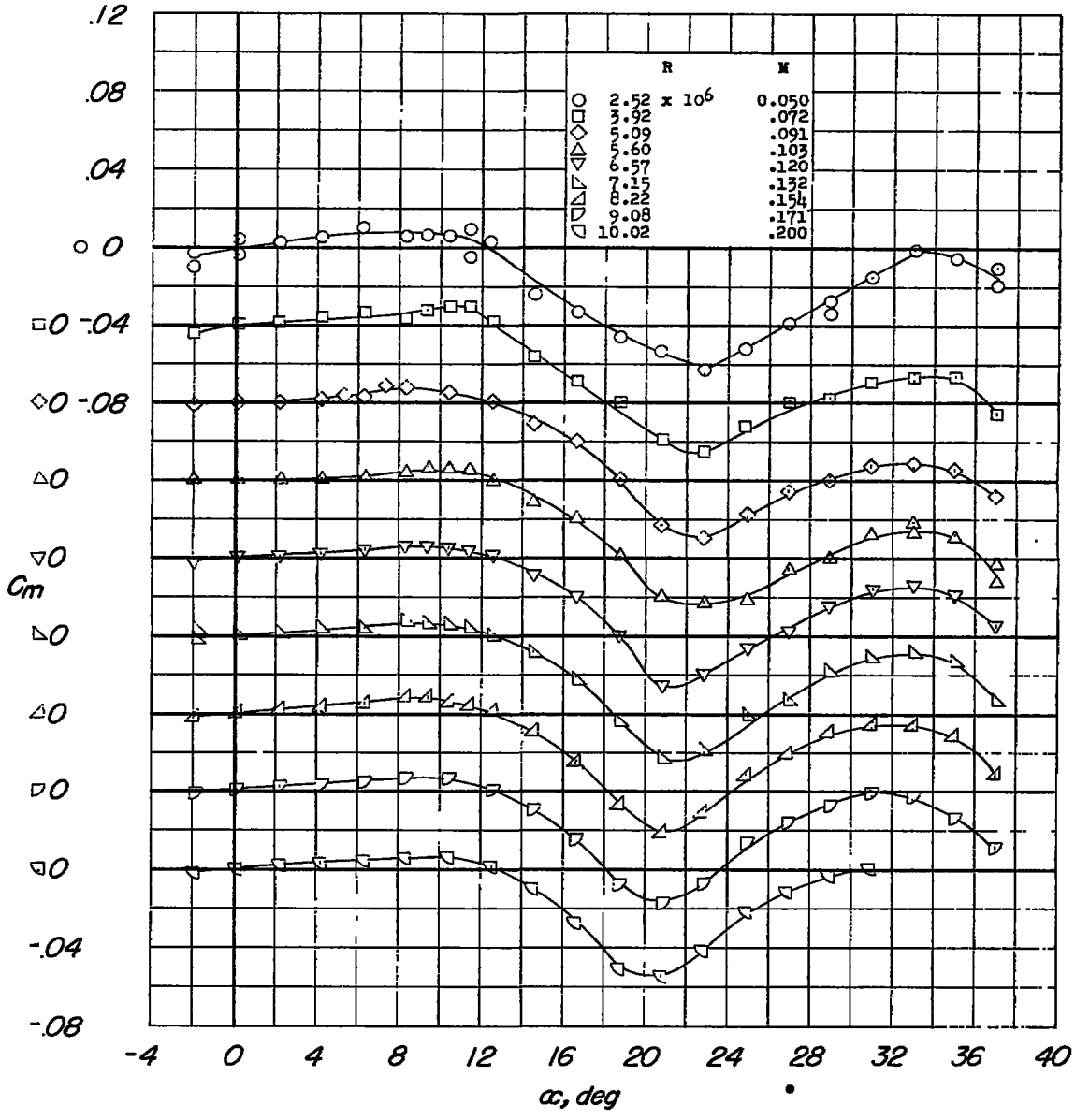

(d) C_m against α; pressure, 33 pounds per square inch.

Figure 5.- Concluded.

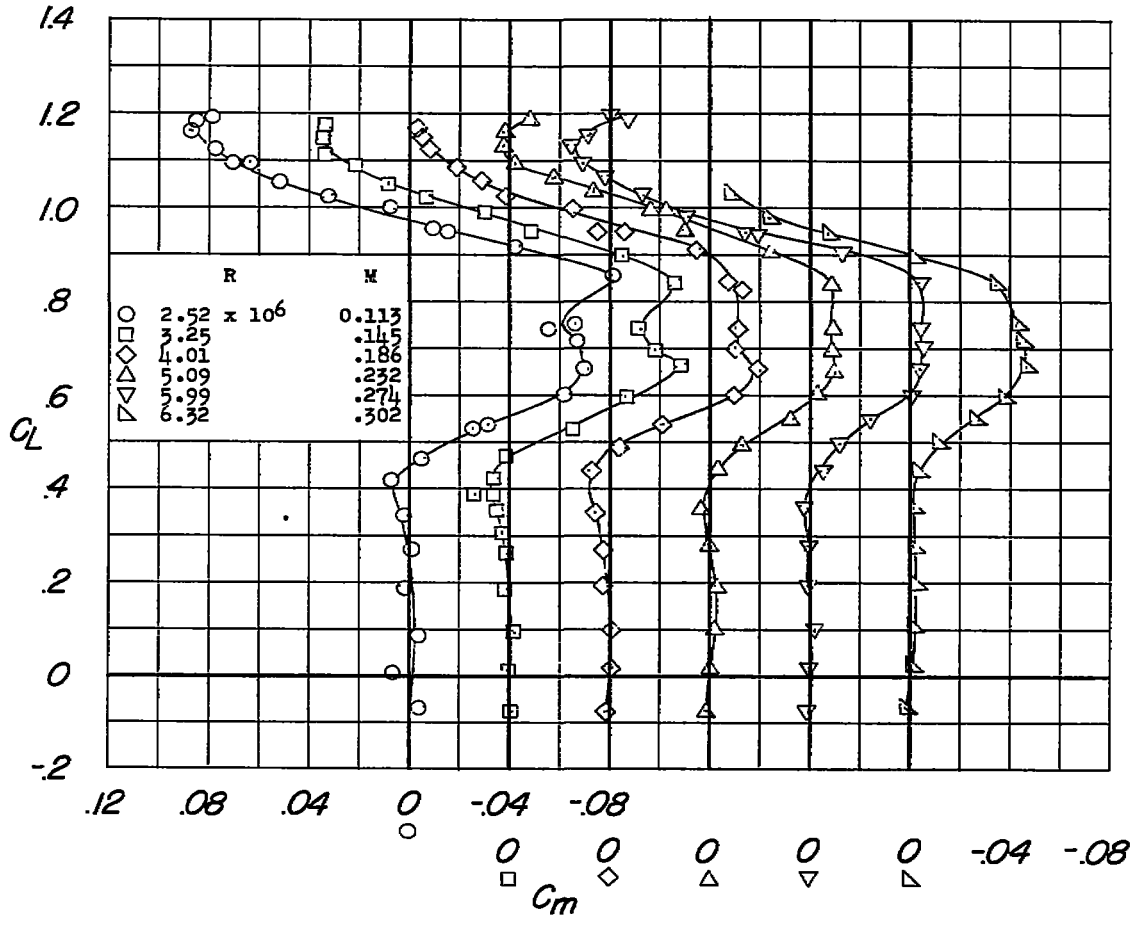

(a) Atmospheric pressure.

Figure 6.- Variation of pitching-moment coefficient with lift coefficient of a 60° sweptback wing. Aspect ratio 3; leading-edge radius 0.0130c.

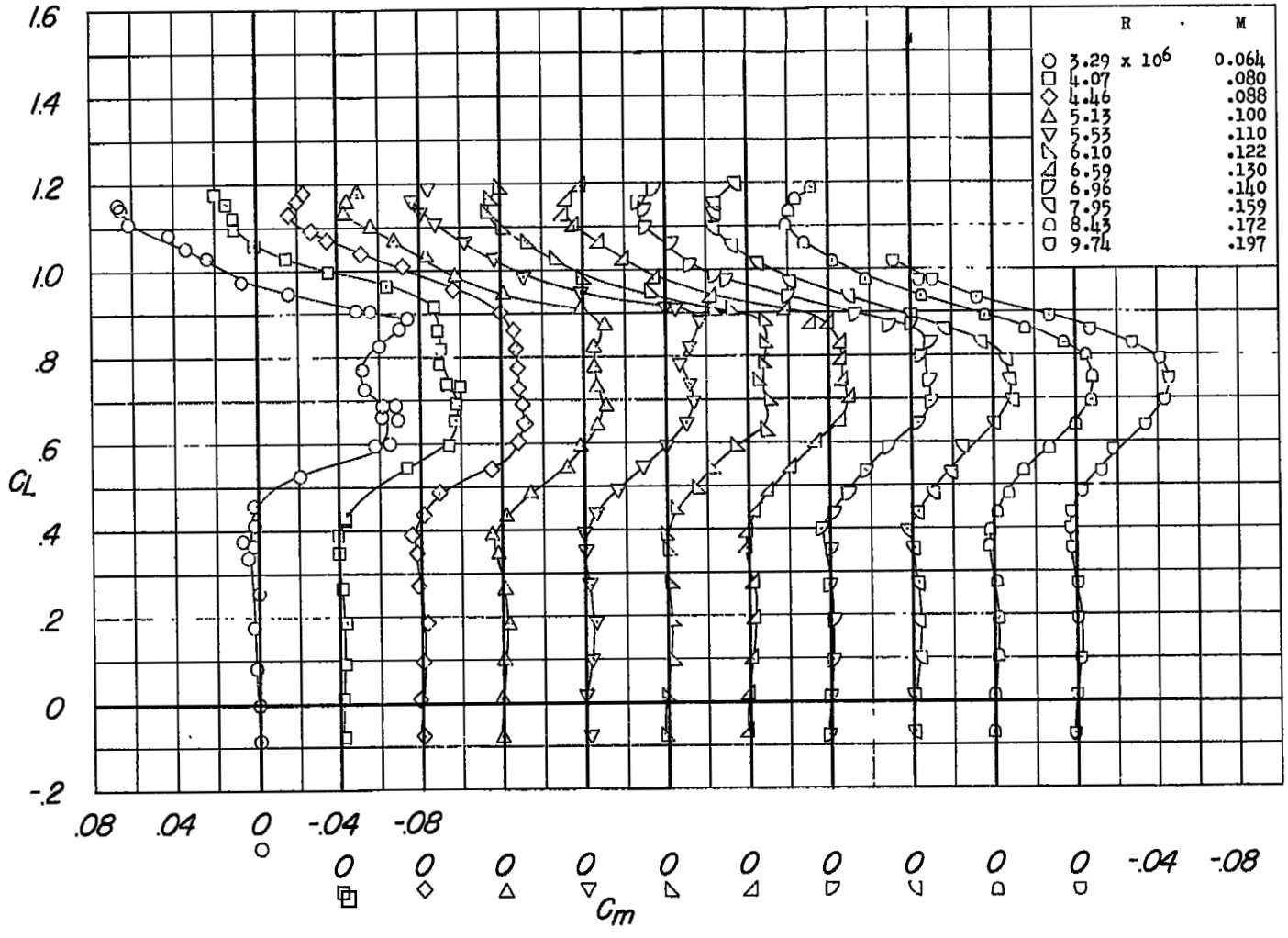

(b) Pressure, 33 pounds per square inch.

Figure 6.- Concluded.

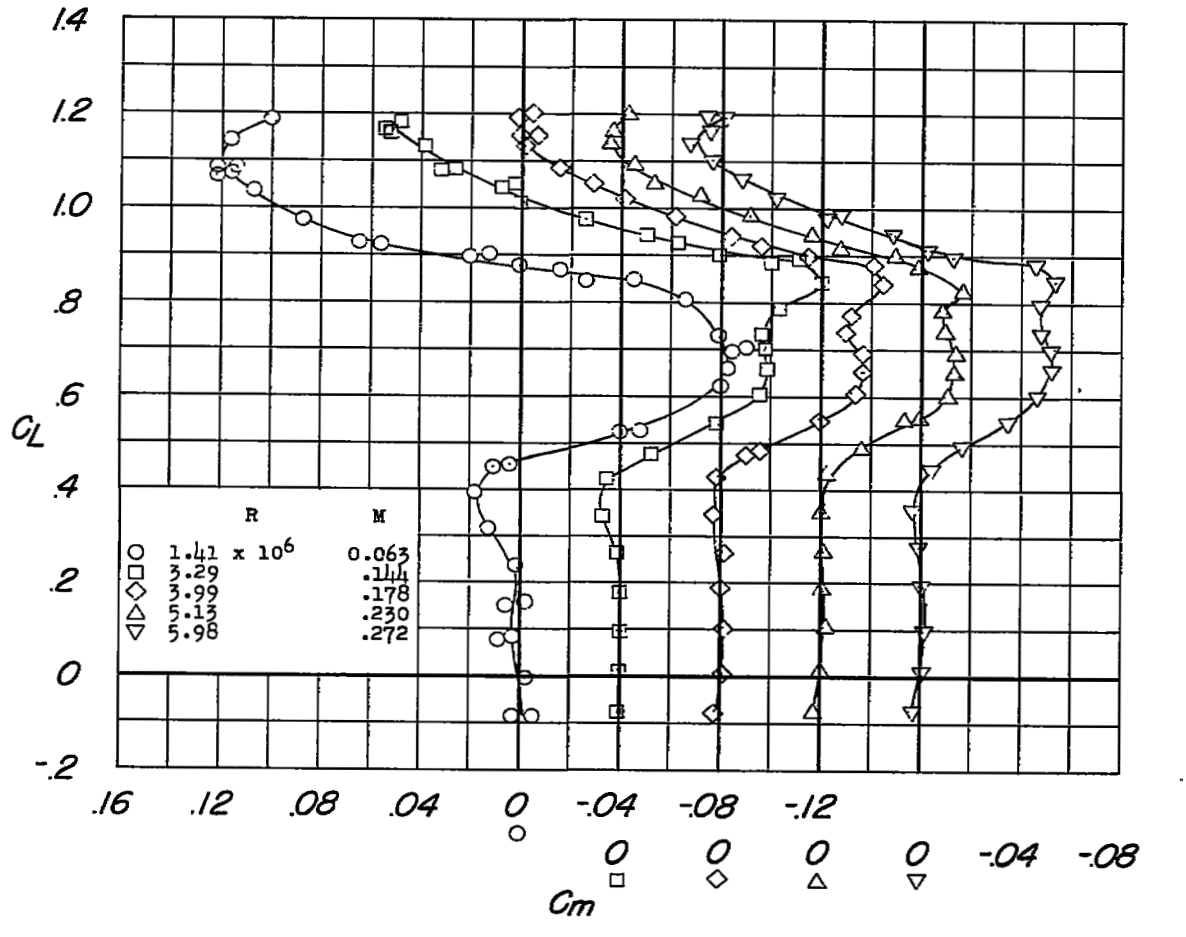

(a) Atmospheric pressure.

Figure 7.- Variation of pitching-moment coefficient with lift coefficient of a 60° sweptback wing. Aspect ratio 3; leading-edge radius 0.0089c.

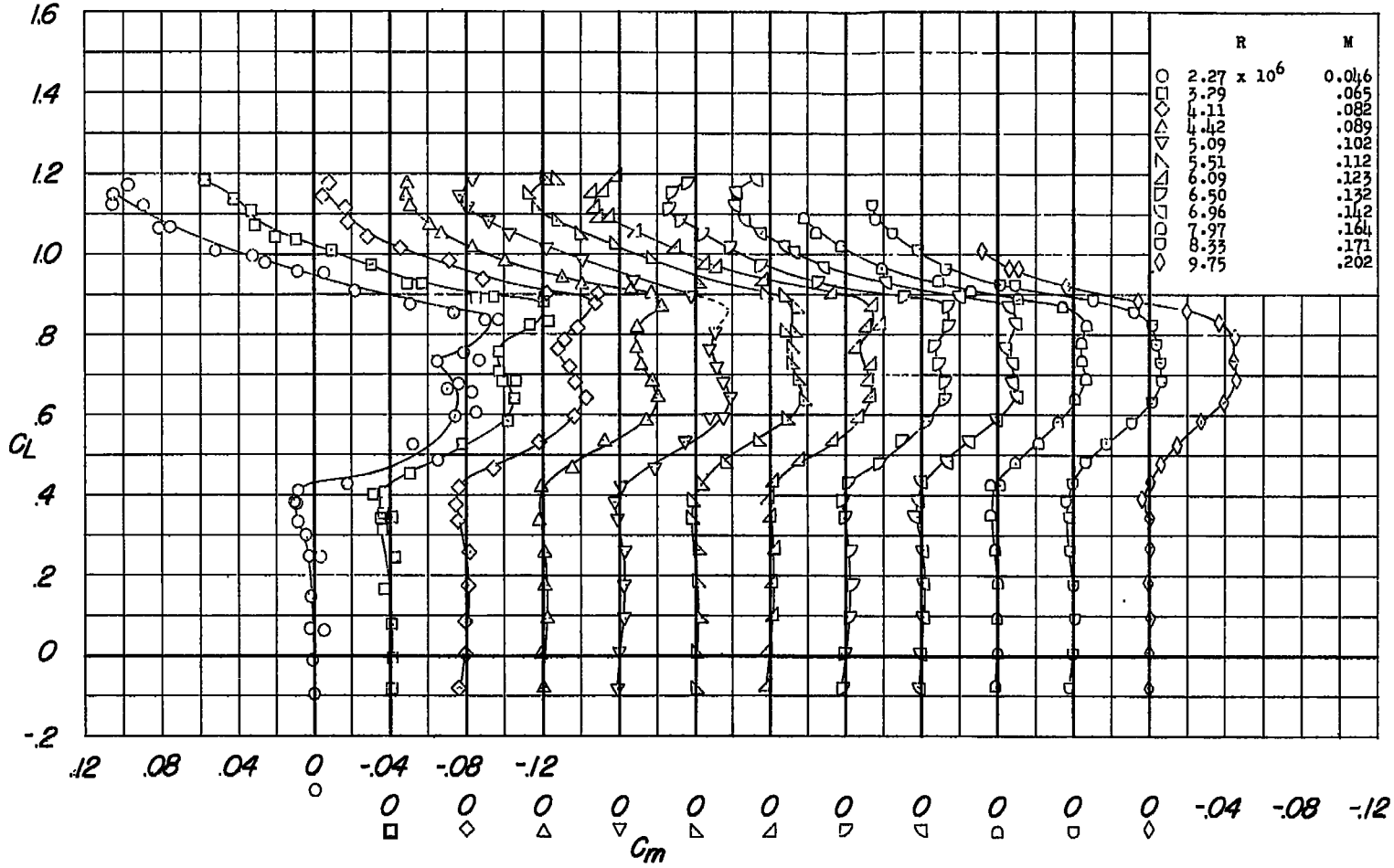

(b) Pressure, 33 pounds per square inch.

Figure 7.- Concluded.

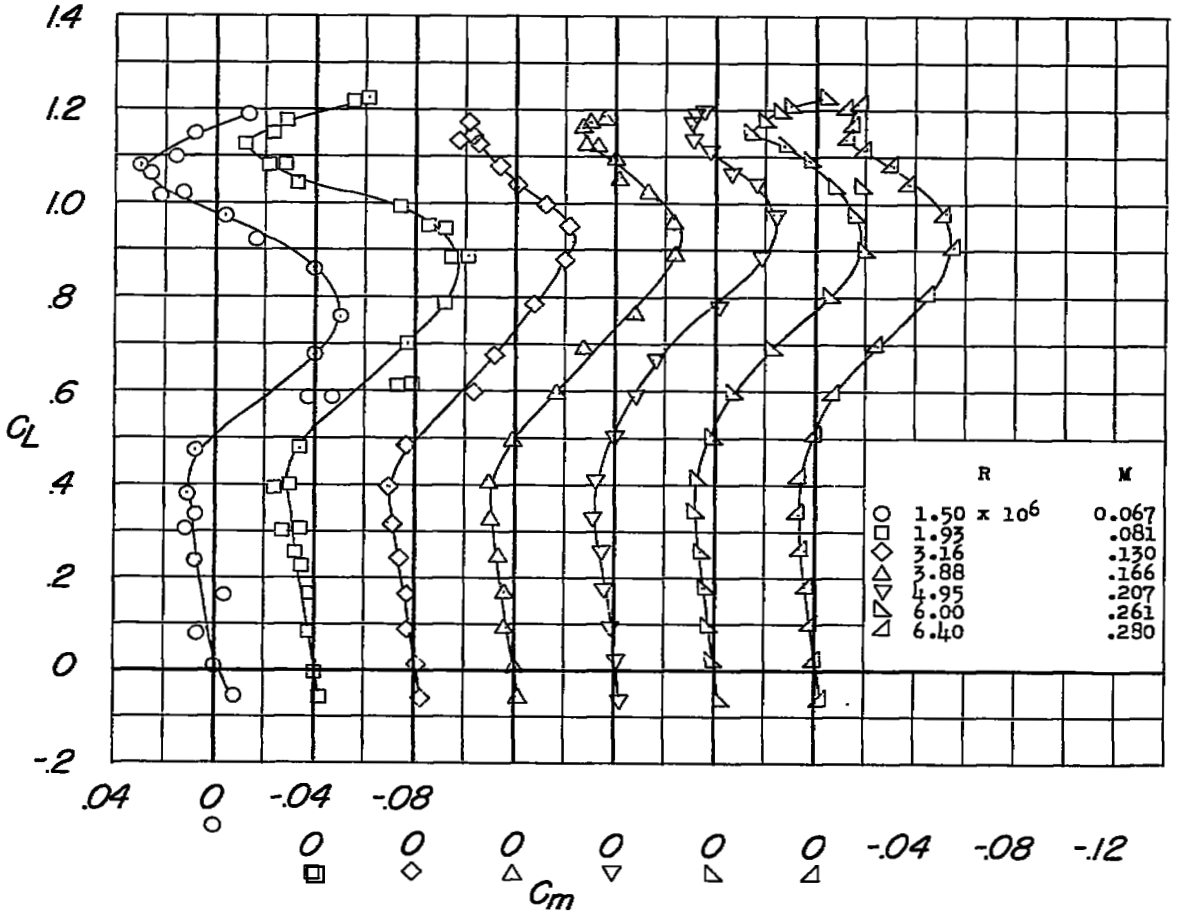

(a) Atmospheric pressure.

Figure 8.- Variation of pitching-moment coefficient with lift coefficient of a 60° sweptback wing. Aspect ratio 2; leading-edge radius 0.0130c.

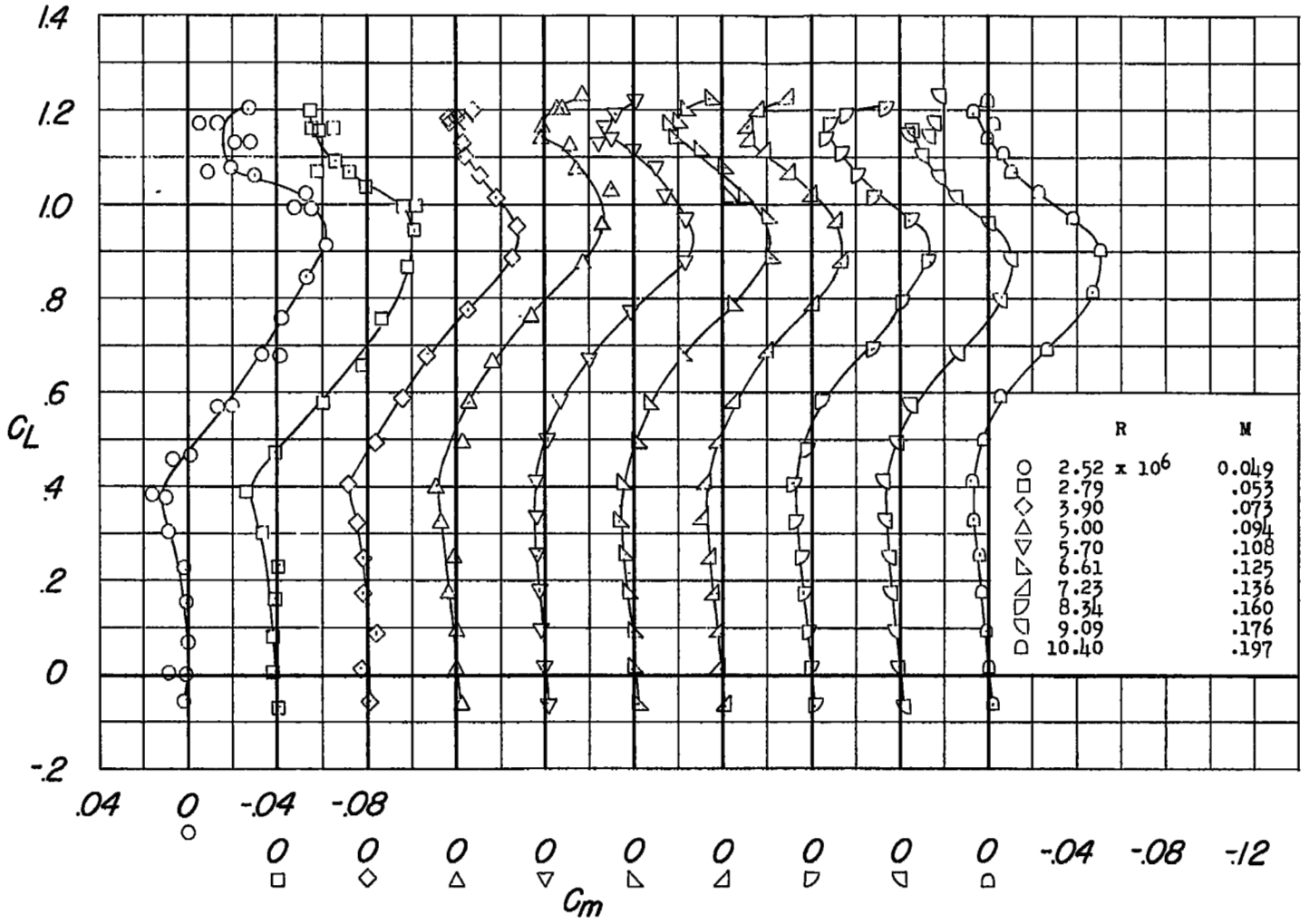

(b) Pressure, 33 pounds per square inch.

Figure 8.- Concluded.

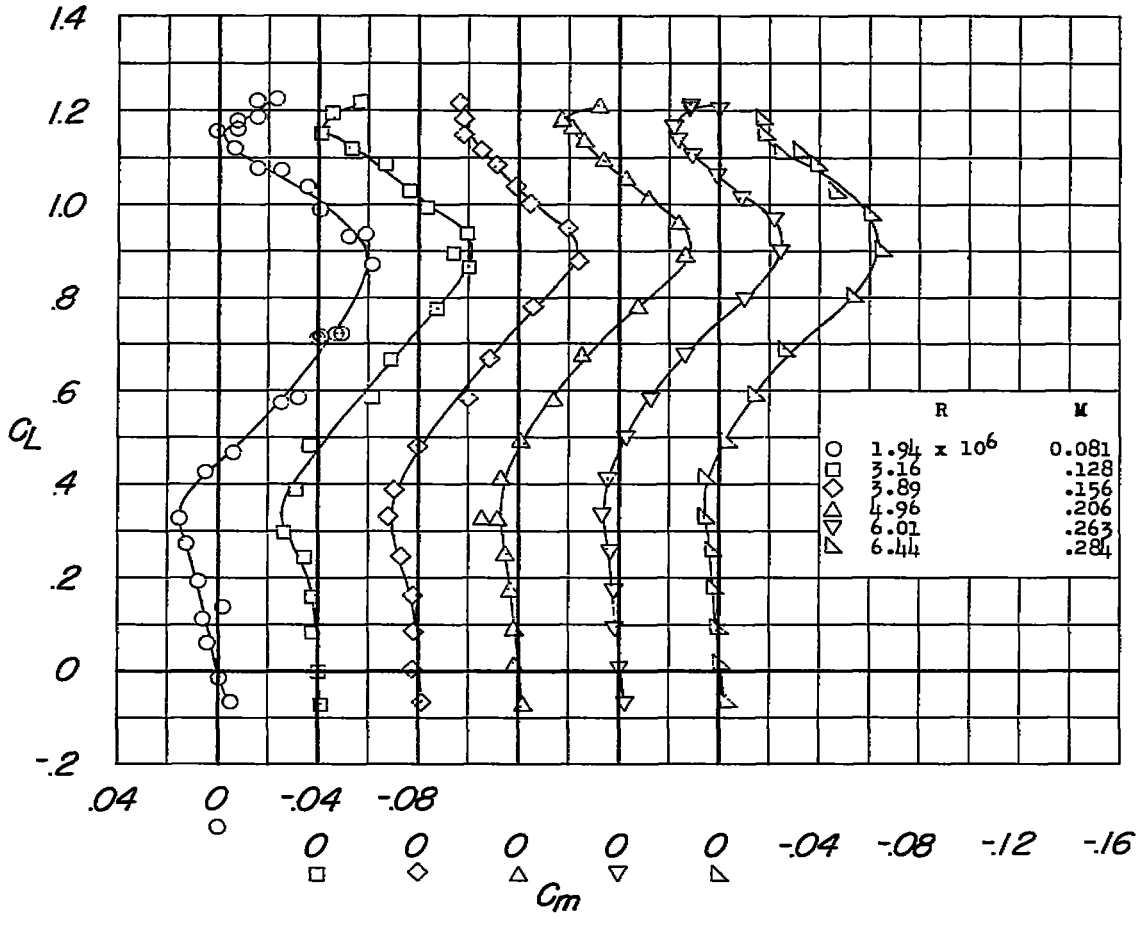

(a) Atmospheric pressure.

Figure 9.- Variation of pitching-moment coefficient with lift coefficient of a 60° sweptback wing. Aspect ratio 2; leading-edge radius 0.0089c.

[redacted]

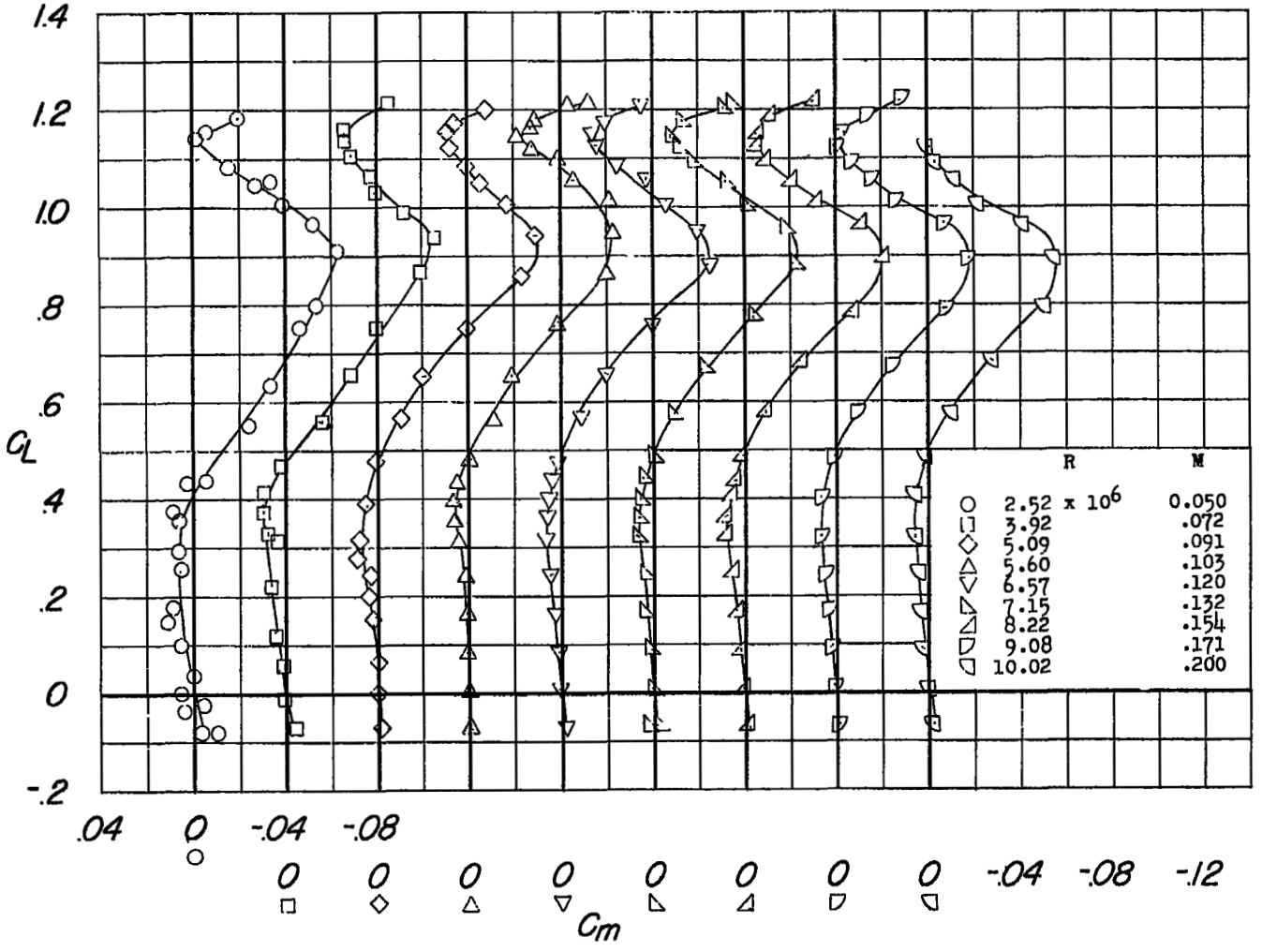

(b) Pressure, 33 pounds per square inch.

Figure 9.- Concluded.

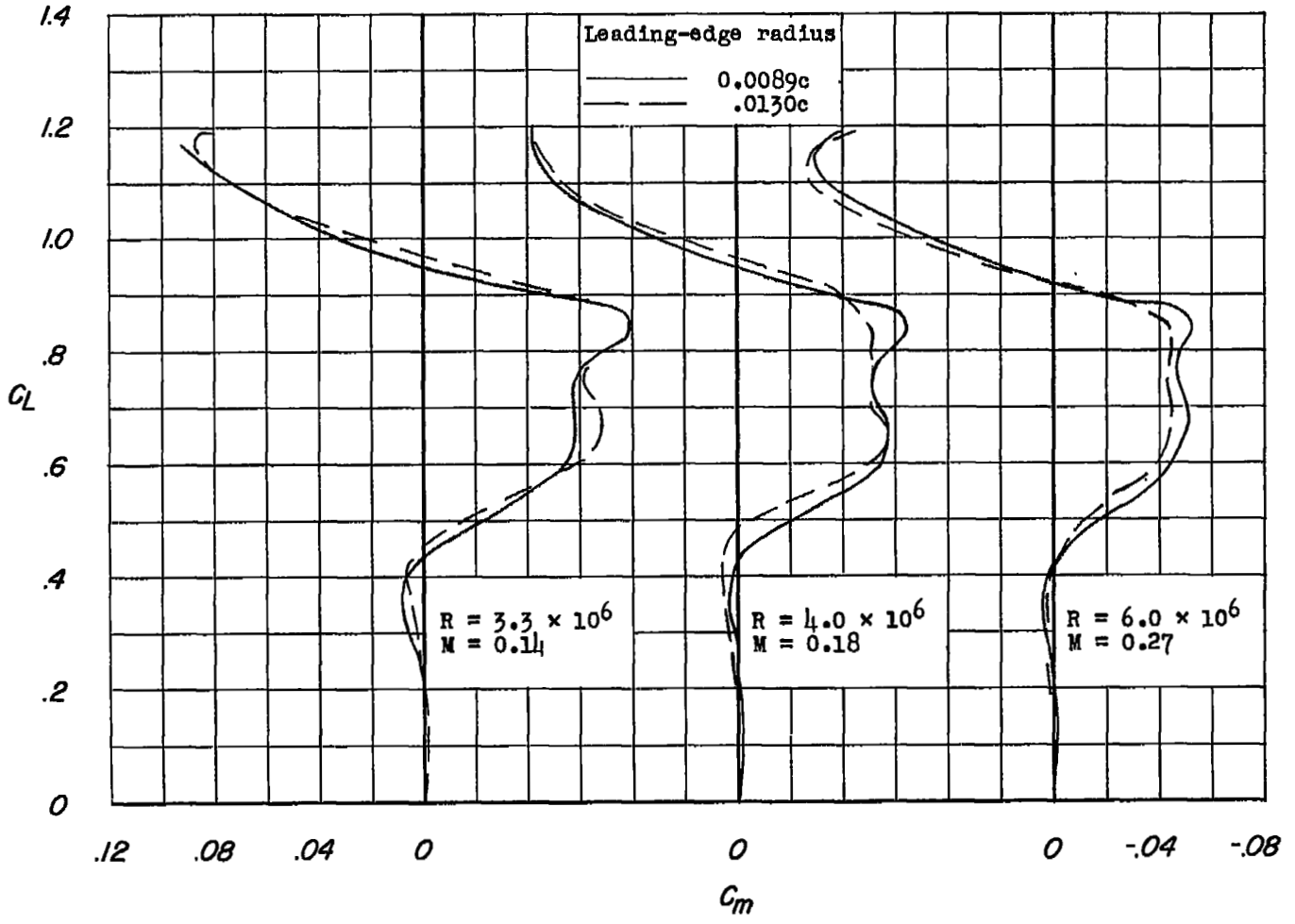

(a) Atmospheric pressure.

Figure 10.- Effect of changes in leading-edge radius from 0.0089c to 0.0130c on the pitching-moment characteristics of a 60° sweptback wing of aspect ratio 3.

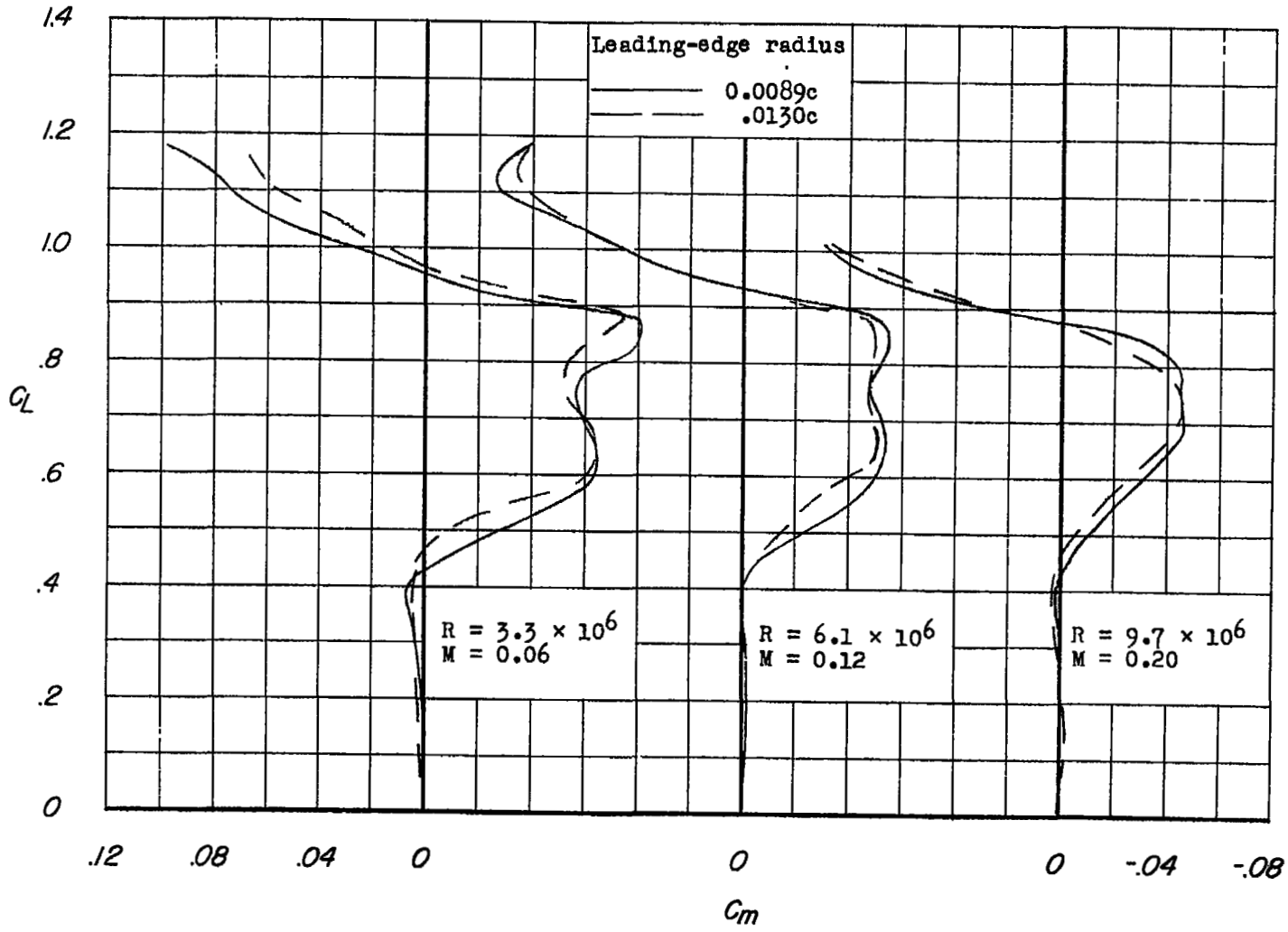

(b) Pressure, 33 pounds per square inch.

Figure 10.- Concluded.

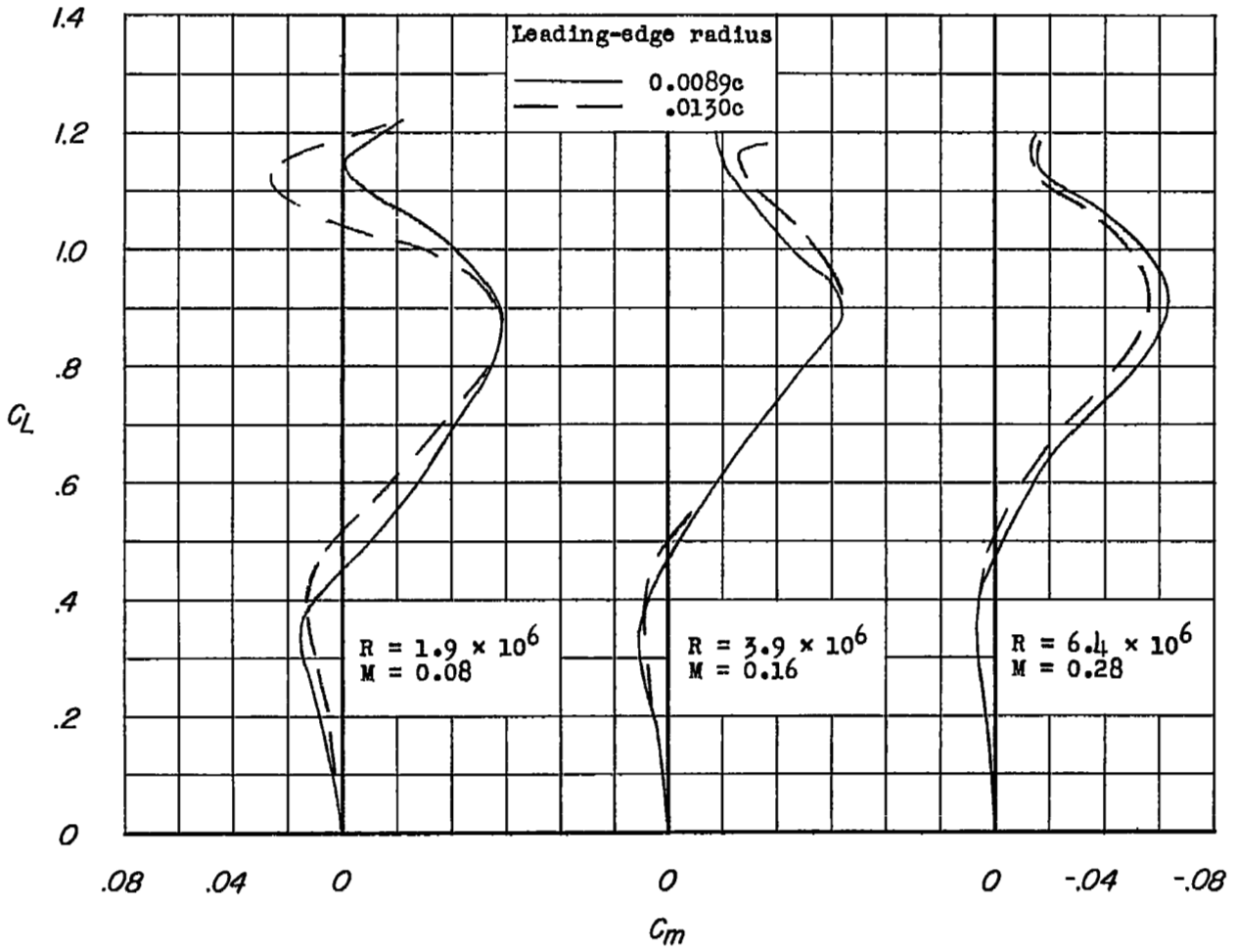

(a) Atmospheric pressure.

Figure 11.- Effect of changes in leading-edge radius from 0.0089c to 0.0130c on the pitching-moment characteristics of a 60° sweptback wing of aspect ratio 2.

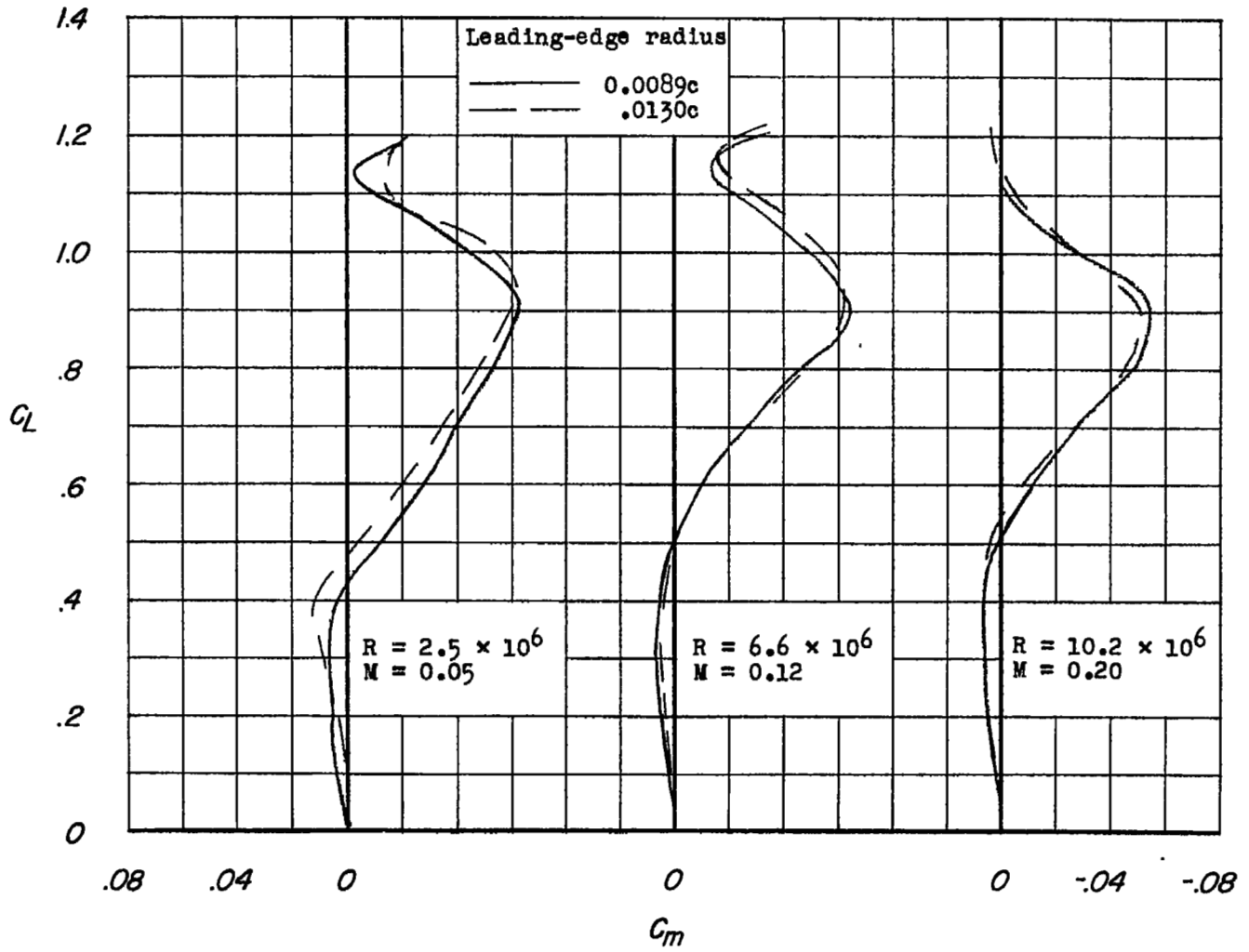

(b) Pressure, 33 pounds per square inch.

Figure 11.- Concluded.

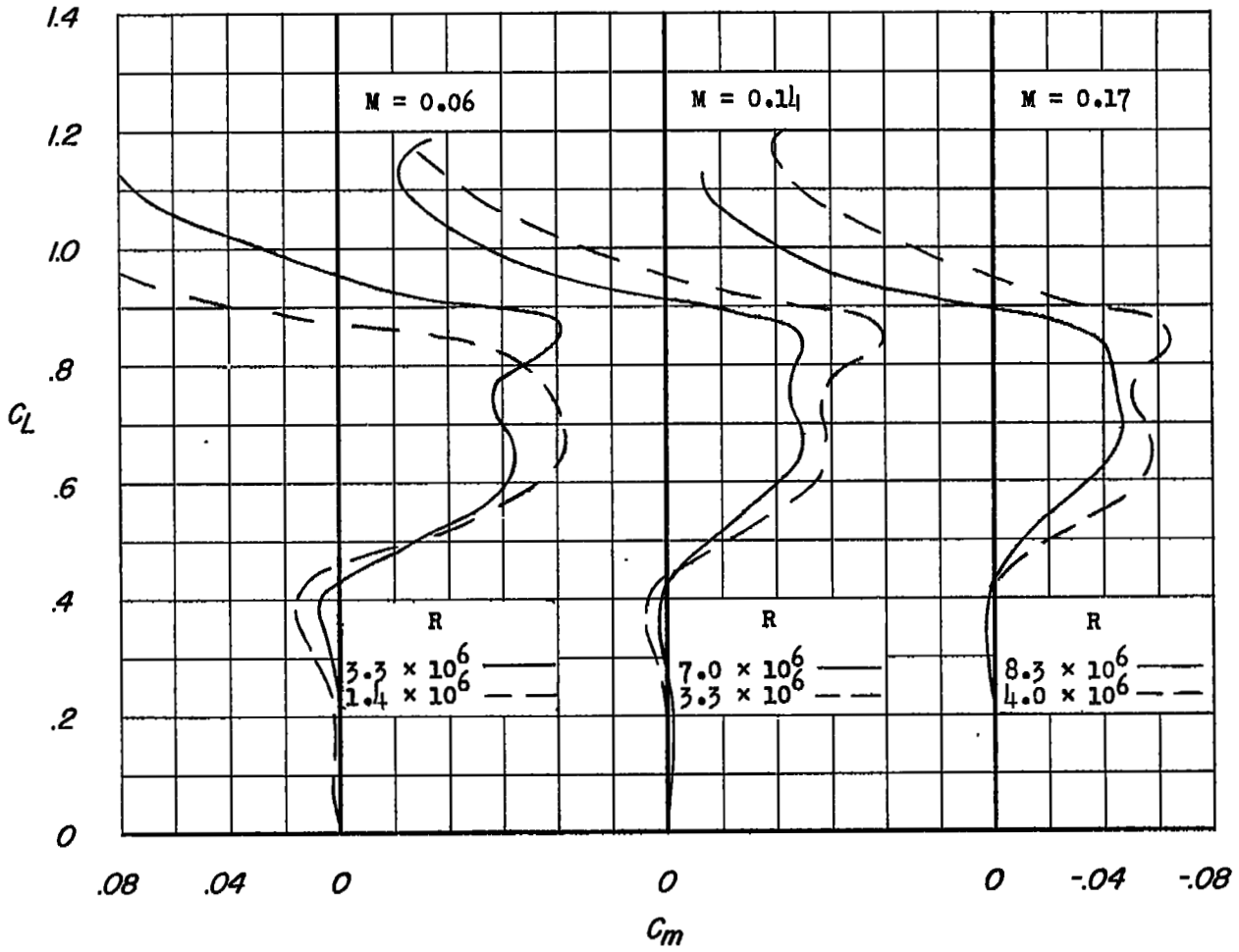

(a) Leading-edge radius 0.0089c.

Figure 12.- Effect of Reynolds number changes on the pitching-moment characteristics of a 60° sweptback wing of aspect ratio 3.

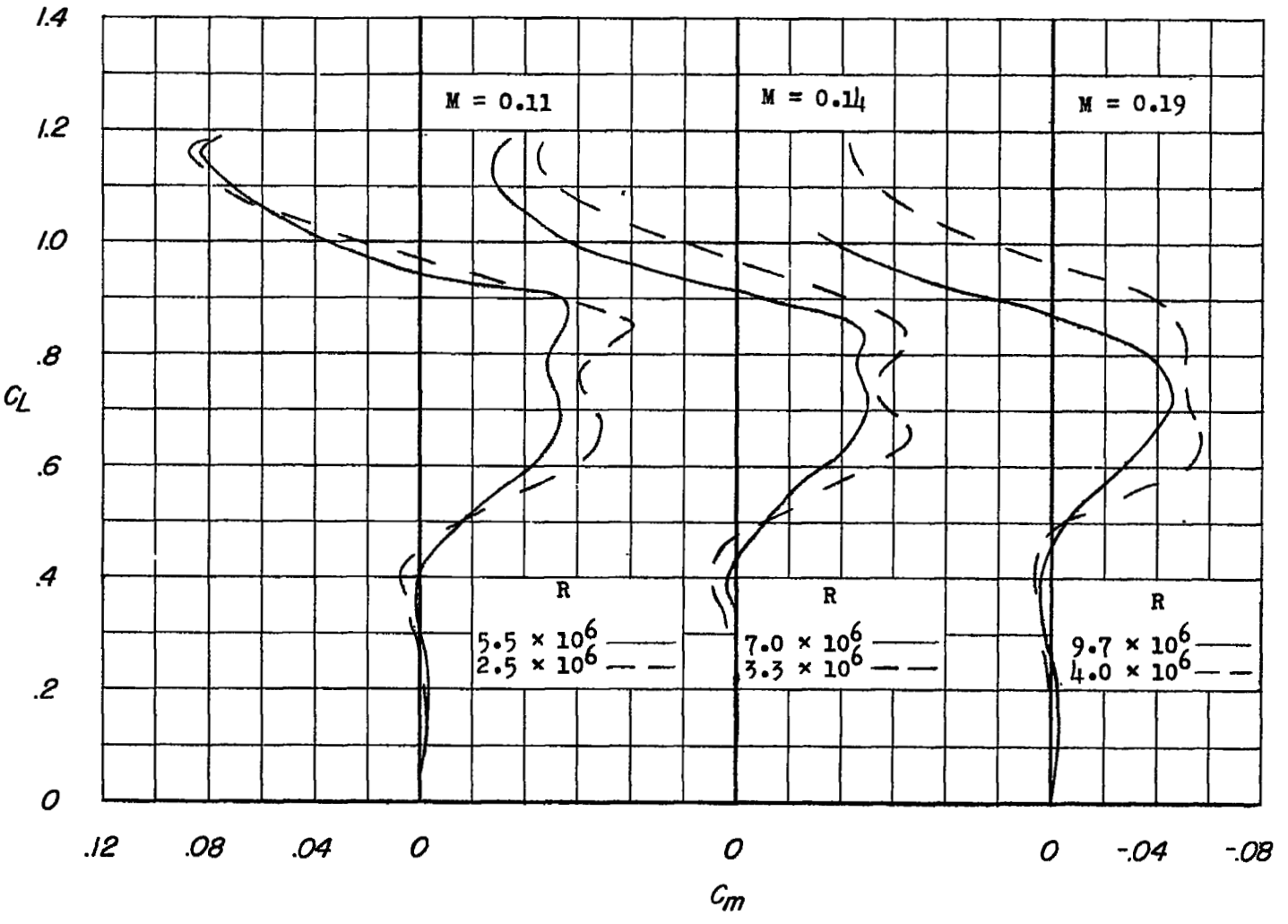

(b) Leading-edge radius 0.0130c.

Figure 12.- Concluded.

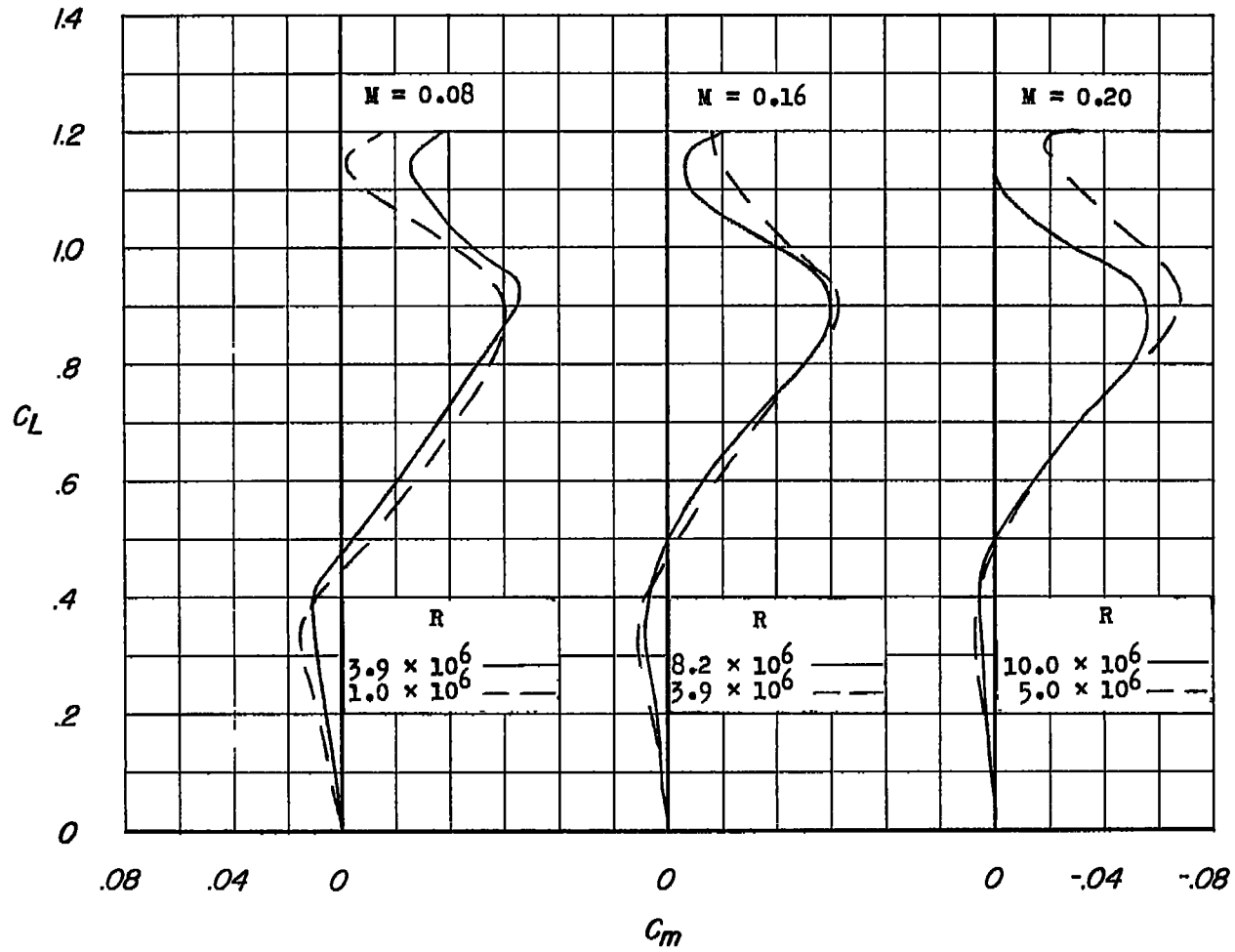

(a) Leading-edge radius 0.0089c.

Figure 13.- Effect of Reynolds number changes on the pitching-moment characteristics of a 60° sweptback wing of aspect ratio 2.

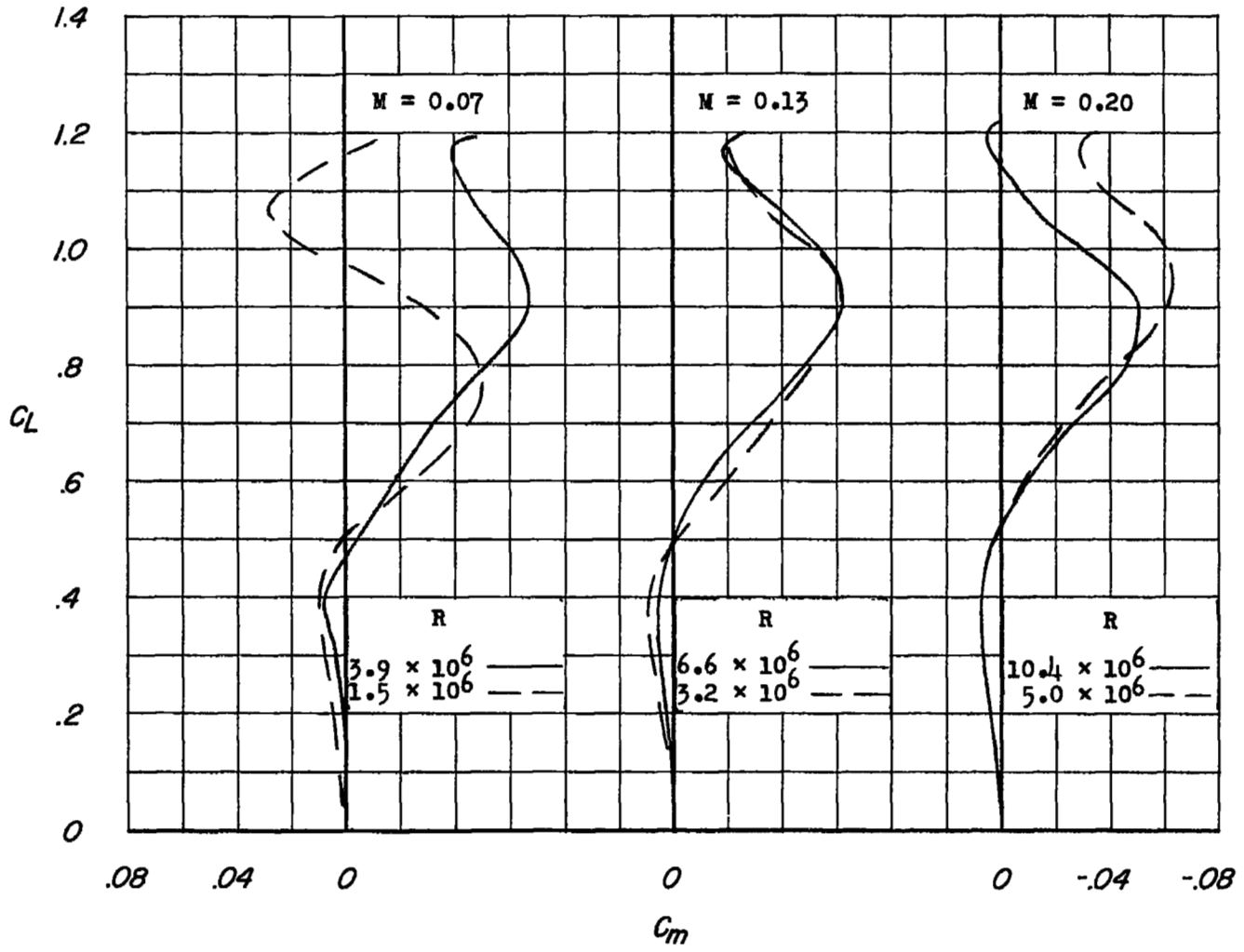

(b) Leading-edge radius 0.0130c.

Figure 13.- Concluded.

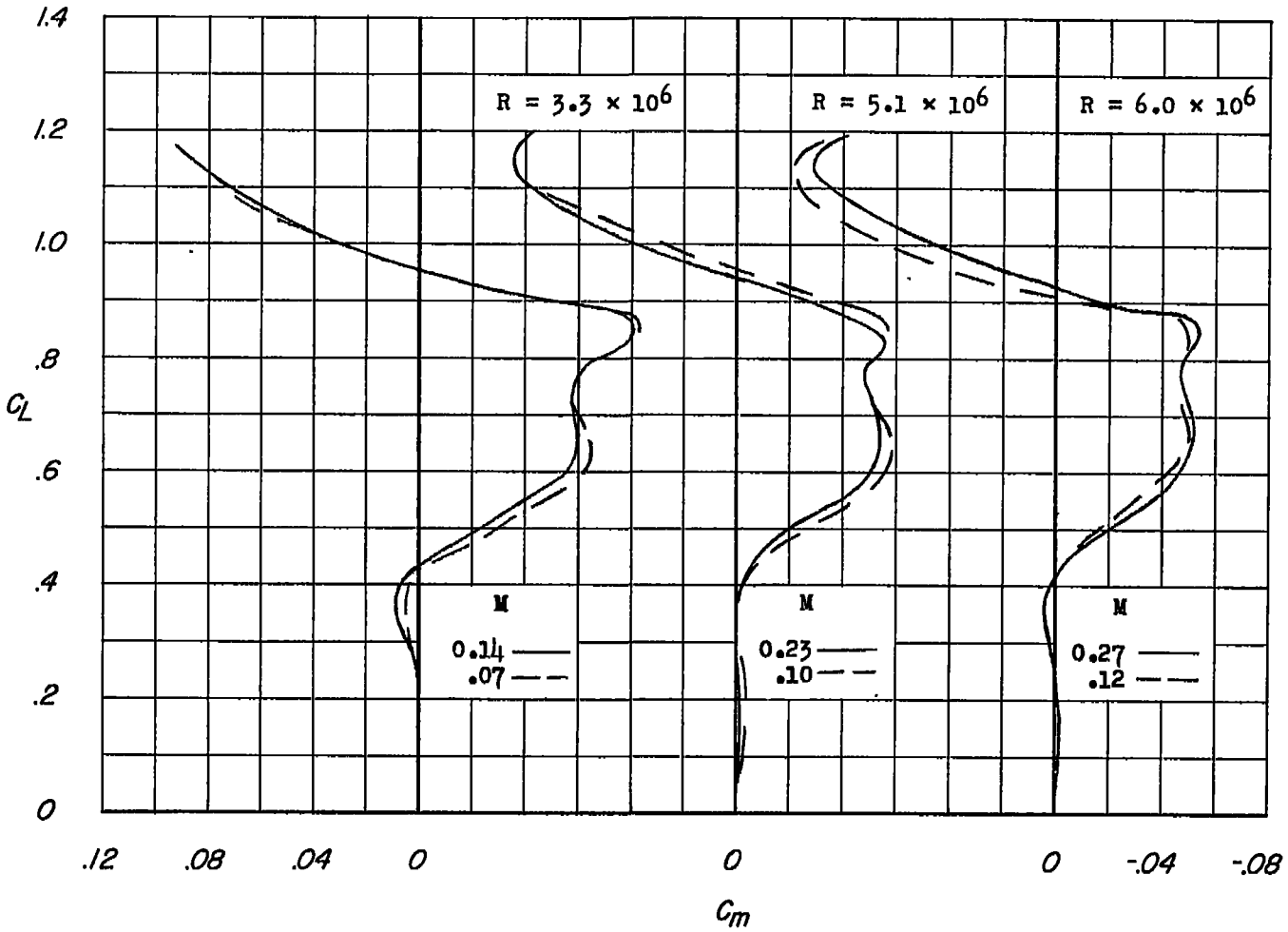

(a) Leading-edge radius 0.0089c.

Figure 14.- Effect of Mach number on the pitching-moment characteristics of a 60° sweptback wing of aspect ratio 3.

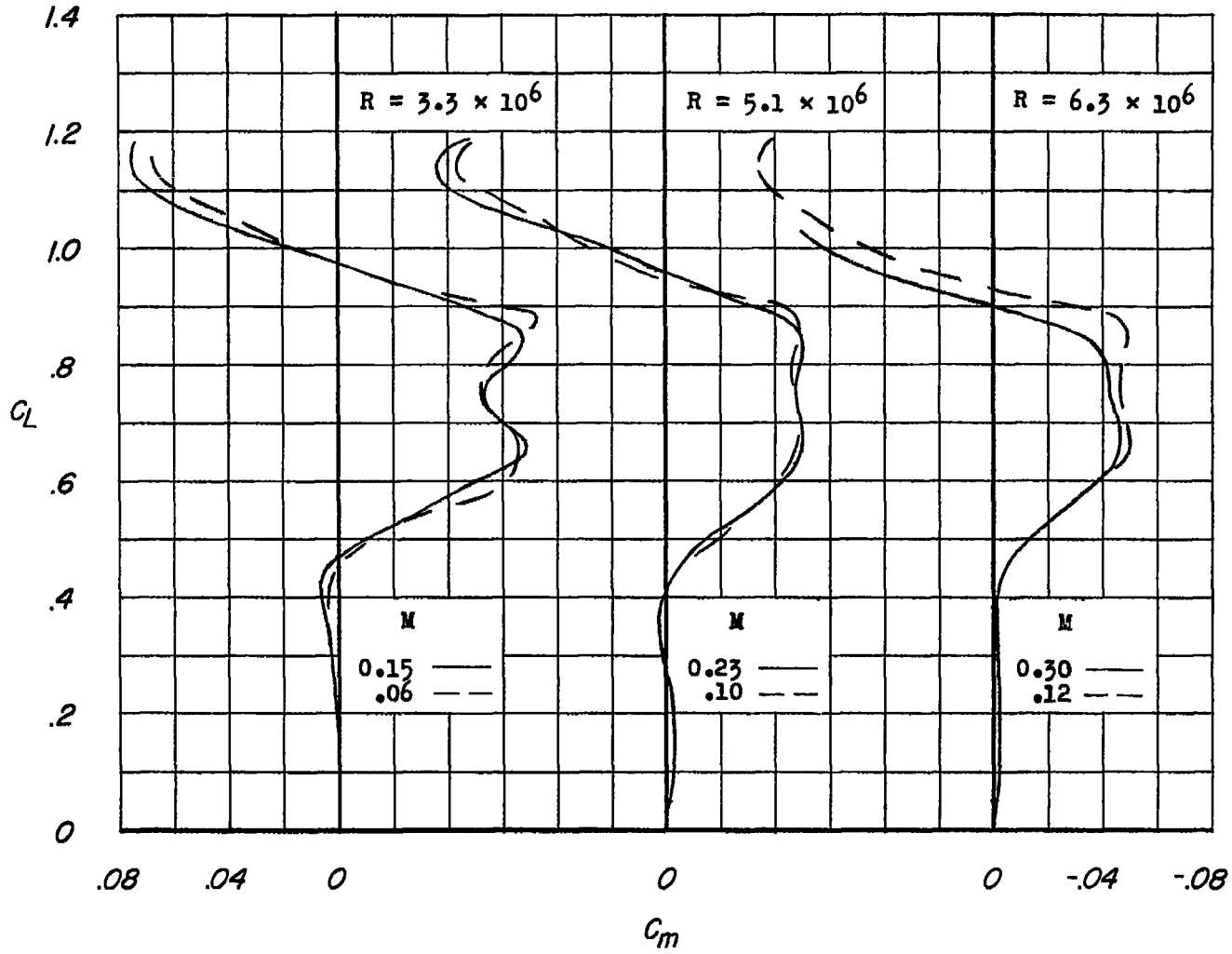

(b) Leading-edge radius 0.0130c.

Figure 14.- Concluded.

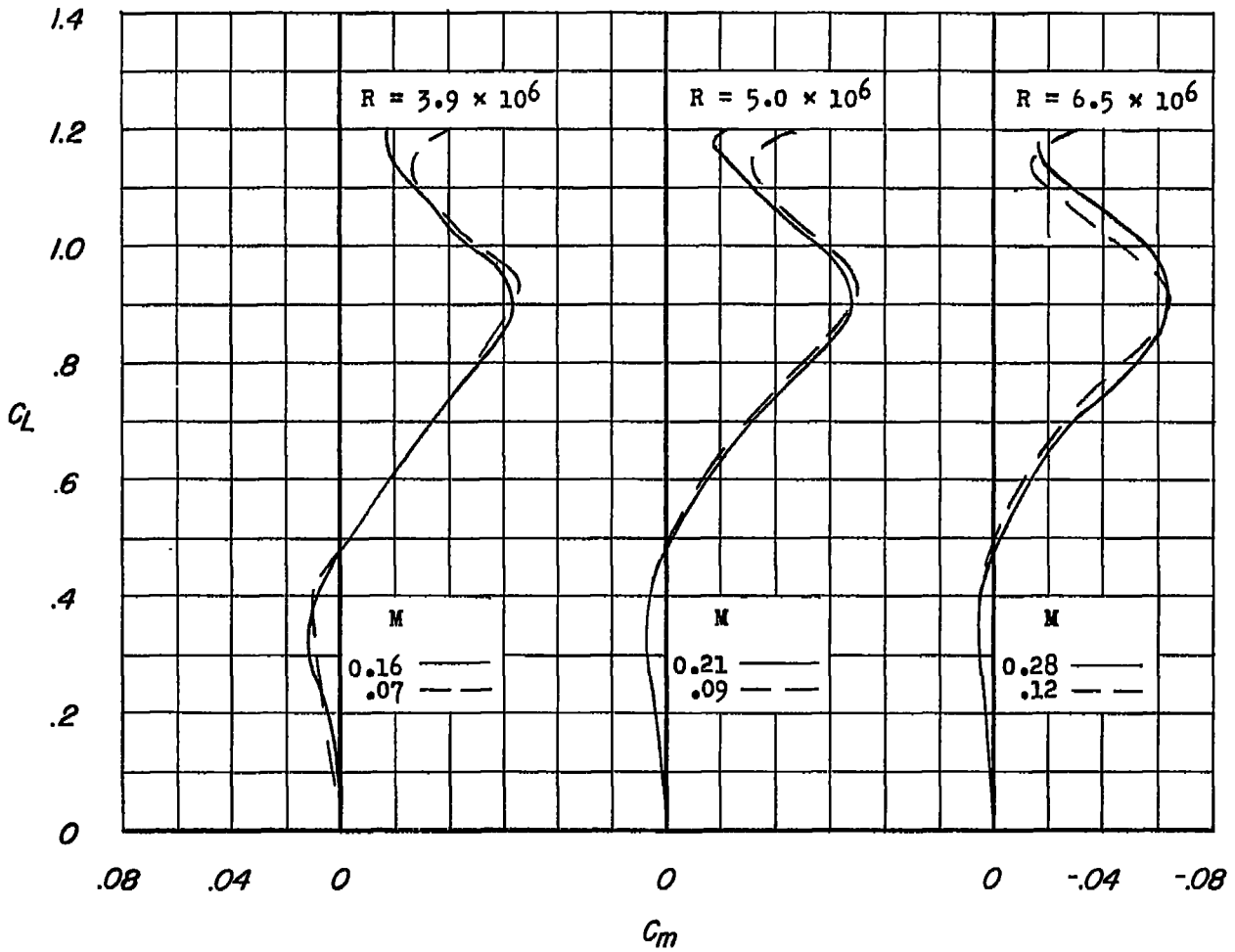

(a) Leading-edge radius 0.0089c.

Figure 15.- Effect of Mach number on the pitching-moment characteristics of a 60° sweptback wing of aspect ratio 2.

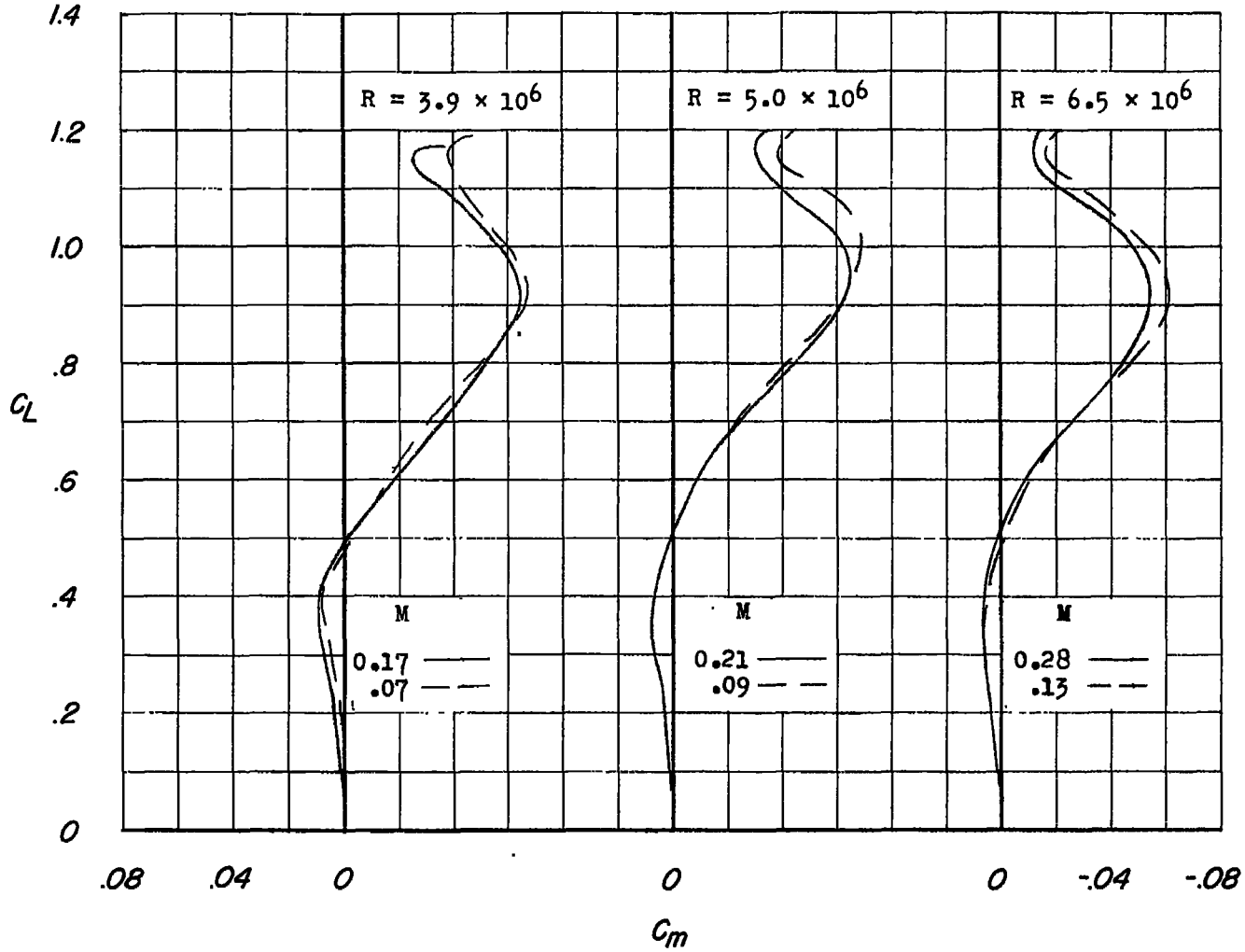

(b) Leading-edge radius 0.0130c.

Figure 15.- Concluded.

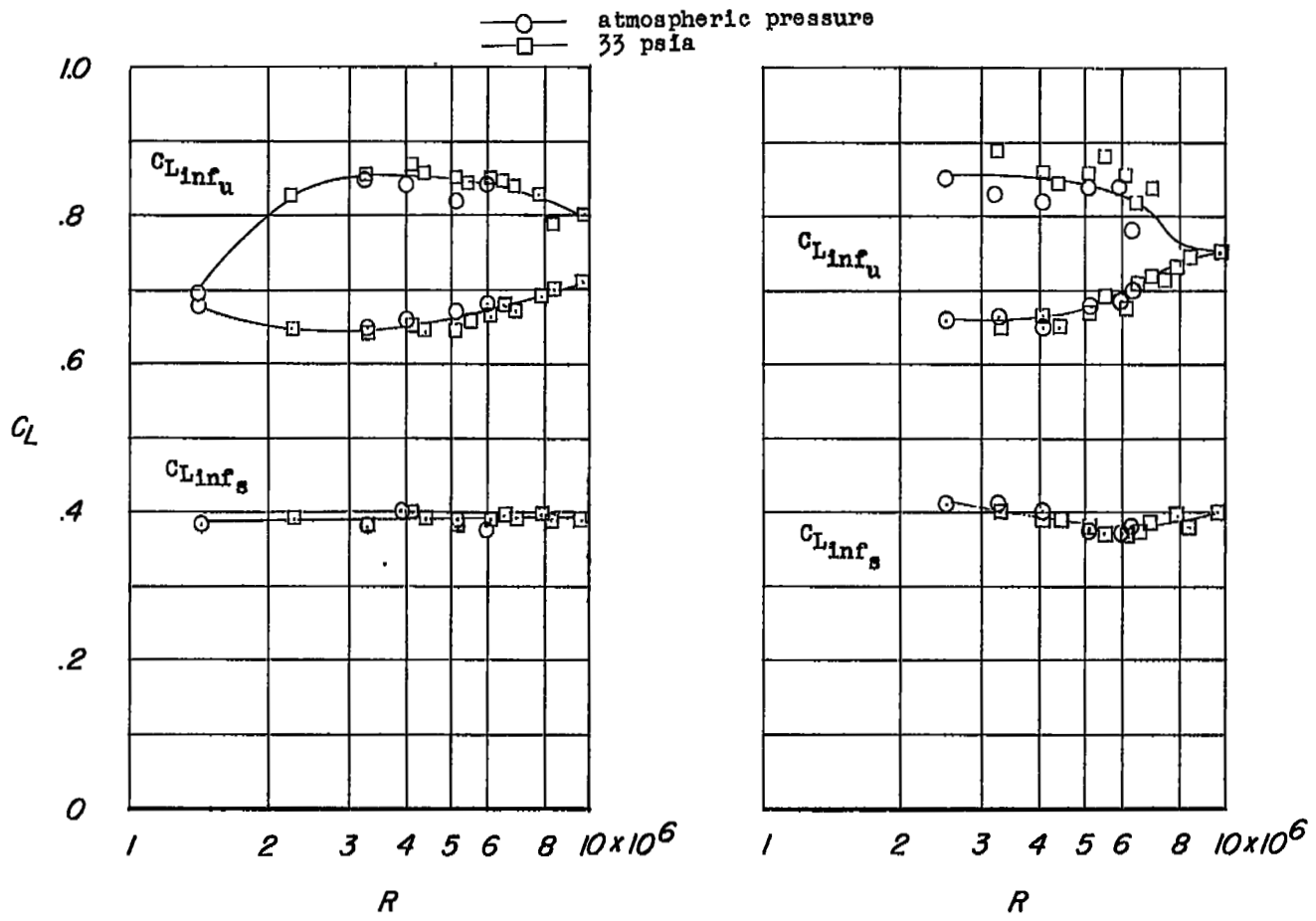

(a) Wing 3-60-89;
leading-edge radius = 0.0089c.

(b) Wing 3-60-130;
leading-edge radius = 0.0130c.

Figure 16.- Variation of inflection lift coefficients with Reynolds number for the wings of aspect ratio 3.

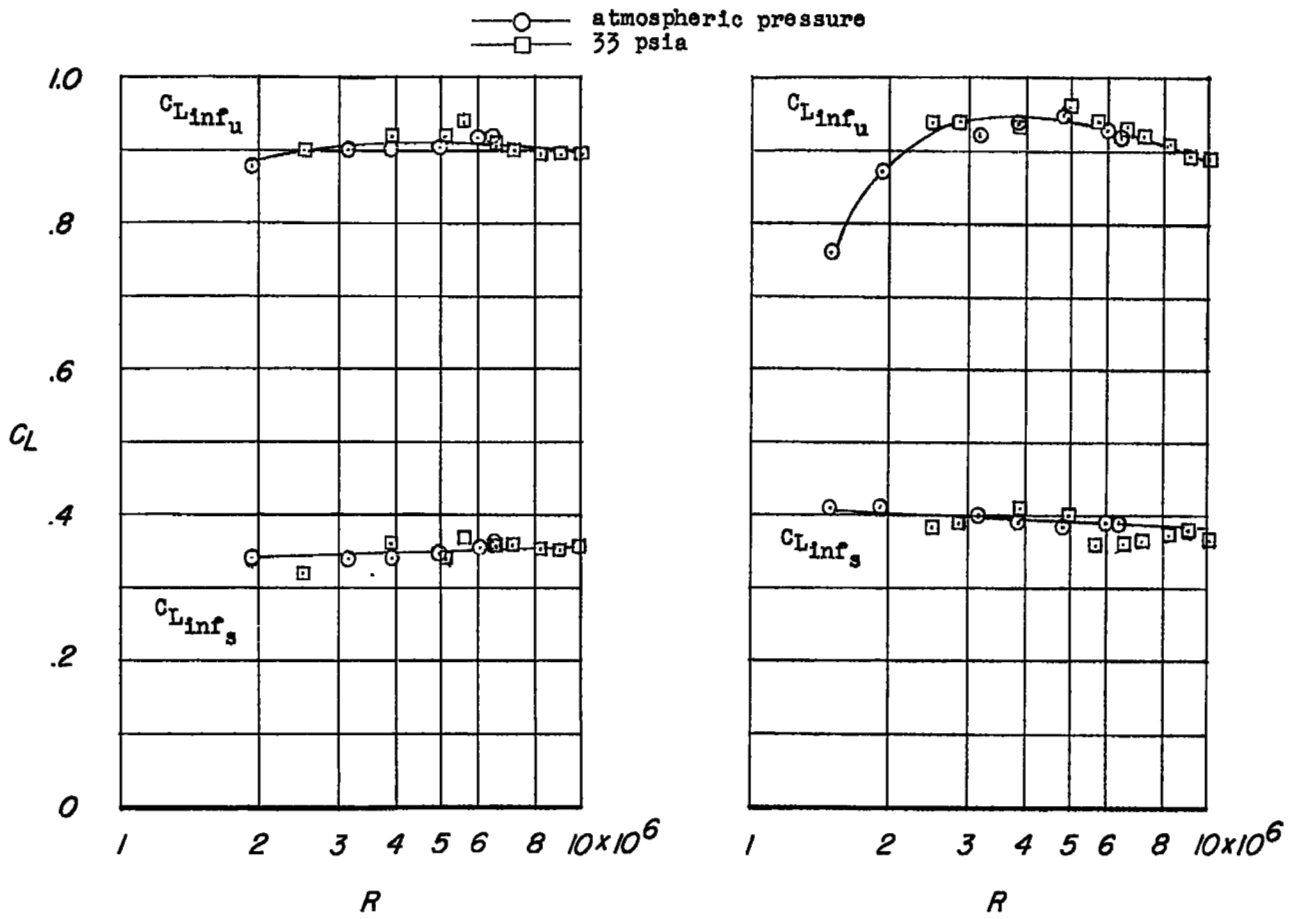

(a) Wing 2-60-89;
leading-edge radius = 0.0089c.

(b) Wing 2-60-130;
leading-edge radius = 0.0130c.

Figure 17.- Variation of inflection lift coefficients with Reynolds number for the wings of aspect ratio 2.